Electron and nuclear dynamics of molecular clusters in ultraintense laser fields. IV. Coulomb explosion of molecular heteroclusters

Isidore Last and Joshua Jortner
School of Chemistry, Tel Aviv University, Ramat Aviv, 69978 Tel Aviv, Israel

(Received 3 June 2004; accepted 11 August 2004)

In this paper we present a theoretical and computational study of the temporal dynamics and energetics of Coulomb explosion of $(CD_4)_n$ and $(CH_4)_n$ $(n=55-4213)$ molecular heteroclusters in ultraintense $(I=10^{16}-10^{19}\,\mathrm{W\,cm^{-2}})$ laser fields, addressing the manifestation of electron dynamics, together with nuclear energetic and kinematic effects on the heterocluster Coulomb instability. The manifestations of the coupling between electron and nuclear dynamics were explored by molecular dynamics simulations for these heteroclusters coupled to Gaussian laser fields (pulse width $\tau=25$ fs), elucidating outer ionization dynamics, nanoplasma screening effects (being significant for $I \leqslant 10^{17}\,\mathrm{W\,cm^{-2}}$), and the attainment of cluster vertical ionization (CVI) (at $I=10^{17}\,\mathrm{W\,cm^{-2}}$ for cluster radius $R_0 \leqslant 31$ Å). Nuclear kinematic effects on heterocluster Coulomb explosion are governed by the kinematic parameter $\eta=q_C m_A/q_A m_C$ for $(CA_4)_n$ clusters $(A=\mathrm{H,D})$, where q_j and m_j $(j=A,\mathrm{C})$ are the ionic charges and masses. Nonuniform heterocluster Coulomb explosion $(\eta>1)$ manifests an overrun effect of the light ions relative to the heavy ions, exhibiting the expansion of two spatially separated subclusters, with the light ions forming the outer subcluster at the outer edge of the spatial distribution. Important features of the energetics of heterocluster Coulomb explosion originate from energetic triggering effects of the driving of the light ions by the heavy ions (C^{4+} for $I=10^{17}-10^{18}\,\mathrm{W\,cm^{-2}}$ and C^{6+} for $I=10^{19}\,\mathrm{W\,cm^{-2}}$), as well as for kinematic effects. Based on the CVI assumption, scaling laws for the cluster size (radius R_0) dependence of the energetics of uniform Coulomb explosion of heteroclusters $(\eta=1)$ were derived, with the size dependence of the average $(E_{j,\mathrm{av}})$ and maximal $(E_{j,\mathrm{M}})$ ion energies being $E_{j,\mathrm{av}}=aR_0^2$ and $E_{j,\mathrm{M}}=(5a/3)R_0^2$, as well as for the ion energy distributions $P(E_j)\propto E_j^{1/2}$; $E_j \leqslant E_{j,\mathrm{M}}$. These results for uniform Coulomb explosion serve as benchmark reference data for the assessment of the effects of nonuniform explosion, where the CVI scaling law for the energetics still holds, with deviations of the a coefficient, which increase with increasing η. Kinematic effects (for $\eta>1$) result in an isotope effect, predicting the enhancement (by 9%–11%) of $E_{\mathrm{H,av}}$ for Coulomb explosion of $(C^{4+}H_4^+)_\eta$ $(\eta=3)$ relative to $E_{\mathrm{D,av}}$ for Coulomb explosion of $(C^{4+}D_4^+)_\eta$ $(\eta=1.5)$, with the isotope effect being determined by the ratio of the kinematic parameters for the pair of Coulomb exploding clusters. Kinematic effects for nonuniform explosion also result in a narrow isotope dependent energy distribution (of width ΔE) of the light ions (with $\Delta E/E_{\mathrm{H,av}} \simeq 0.3$ and $\Delta E/E_{\mathrm{D,av}} \simeq 0.4$), with the distribution peaking at the high energy edge, in marked contrast with the uniform explosion case. Features of laser-heterocluster interactions were inferred from the analyses of the intensity dependent boundary radii $(R_0)_I$ and the corresponding average D^+ ion energies $(E_{\mathrm{D,av}})_I$, which provide a measure for optimization of the cluster size at intensity I for the neutron yield from dd nuclear fusion driven by Coulomb explosion (NFDCE) of these heteroclusters. We infer on the advantage of deuterium containing heteronuclear clusters, e.g., $(CD_4)_n$ in comparison to homonuclear clusters, e.g., $(D_2)_{n/2}$, for dd NFDCE, where the highly charged heavy ions (e.g., C^{4+} or C^{6+}) serve as energetic and kinematic triggers driving the D^+ ions to a high (10–200 keV) energy domain. © *2004 American Institute of Physics.* [DOI: 10.1063/1.1802554]

I. INTRODUCTION

Of considerable interest is the electron and nuclear dynamics of elemental and molecular clusters, e.g., $(Xe)_n$,[1–17] $(D_2)_n$, and $(H_2)_n$,[18–26] $(D_2O)_n$,[20–22,27] and $(CD_4)_n$,[28,29] in ultraintense laser fields. The response of clusters to ultraintense laser fields $(I=10^{15}-10^{20}\,\mathrm{W\,cm^{-2}})$ is distinct both from the electron dynamic response in ordinary fields $(I \lesssim 10^{13}\,\mathrm{W\,cm^{-2}})$, where perturbative quantum electrodynamics is applicable, and from the response of ''small'' atoms or molecules to ultraintense laser fields, which is triggered by the barrier suppression single-step ionization mechanism.[30–32] When the cluster size (or the size of a large chemical system) significantly exceeds the size of the constituent barrier distance, a compound cluster ionization mechanism is manifested, which occurs via sequential-simultaneous, inner-outer ionization processes.[6,8,30–33] The electron dynamic processes trigger nuclear dynamics, with the outer ionization being accompanied by cluster Coulomb

explosion, which results in the production of highly energetic (keV–MeV) multicharged ions on the ultrashort (10–100 fs) time scale.[6,8,21,34,35]

Recent applications of Coulomb explosion in highly charged clusters pertain to Coulomb explosion imaging[36,37] and to spatial resolution of reaction dynamics.[38–40] An interesting development in this field involves *dd* nuclear fusion driven by Coulomb explosion (NFDCE) of deuterium containing homonuclear $(D_2)_{n/2}$ clusters and of heteronuclear $(D_2O)_n$ and $(CD_4)_n$ clusters, for which compelling experimental[18,19,25,29] and theoretical[20–22,24,28,31] evidence became available.

Early theoretical studies of Coulomb explosion of molecular clusters rested on some approximate methods, which separated electron and nuclear dynamics. The cluster vertical ionization (CVI) approximation[14,21,30,35,41,42] separated the time scales of the fast electron dynamics and the slower nuclear dynamics. The sudden inner cluster ionization (SICI) approximation implies that at the onset of outer ionization and Coulomb explosion, the inner ionization process is complete.[6,21,28]

Transcending the CVI and SICI approximations, progress was recently made in the understanding of the coupling between electron and nuclear dynamics in the Coulomb explosion of homonuclear deuterium molecular clusters. In our recent studies of deuterium $(D_2)_{n/2}$, deuterated methane $(CD_4)_n$, and xenon Xe_n clusters in ultraintense laser fields[32,33,42] (referred to as Papers I, II, and III, respectively), we explored important features of the electron and nuclear dynamics in the coupled laser-cluster system. By the studies of the effects of laser intensity, pulse shape width, and frequency, as well as cluster size effects on Coulomb explosion of homonuclear $(D_2)_{n/2}$ clusters, we elucidated the effects of electron dynamics on nuclear dynamics as manifested by the energetics and angular distribution of the ions (Paper III).

It will be interesting to extend these studies of electron-nuclear coupling in Coulomb explosion and NFDCE of molecular heteroclusters. In this paper we study Coulomb explosion in molecular heteroclusters of methane $(CH_4)_n$ and deuterated methane $(CD_4)_n$ $(n=55-4213)$ in ultraintense $(I=10^{16}-10^{19}\,\mathrm{W\,cm^{-2}})$ laser fields using classical dynamics simulation methods (Paper I). Coulomb explosion of $(CH_4)_n$, $(CD_4)_n$, and $(CT_4)_n$ clusters was already studied by us[28] on the basis of the SICI approximation, utilizing truncated Gaussian laser pulses.[14] In this paper we explore the manifestations of the coupling between electronic and nuclear dynamics in these heteroclusters coupled to realistic laser pulses. From the time-resolved dynamics and energetics of Coulomb explosion of heteroclusters induced by Gaussian laser pulses (Paper I) we shall infer on the validity range of the pseudo-CVI domain for the intensity dependent boundary radii $(R_0)_I$ and the average ion energies $(E_{\mathrm{av}})_I$ (Paper III) in the Coulomb explosion of methane heteroclusters. The scaling relation $E_{\mathrm{av}} \propto R_0^2$ for the pseudo-CVI domain previously advanced and explored for Coulomb explosion of homonuclear clusters (Paper III) will now be extended for Coulomb instability of heteronuclear clusters. While Coulomb explosion of homonuclear clusters is uniform (Paper III), Coulomb explosion of heteroclusters can either be uniform or nonuniform, depending on the kinematic parameter.[20,21,28] We shall show that the dynamics and energetics of uniformly exploding heteroclusters can be expressed in terms of analytical expressions for the scaling laws, while for nonuniformly exploding clusters important features are manifested in isotope effects on the energetics. Subsequently, we shall provide quantitative results for the enhancement of the energies of the D^+ ions driven by Coulomb explosion of $(CD_4)_n$ heteroclusters, relative to the energetics of Coulomb explosion of homonuclear $(D_2)_{n/2}$ clusters of the same size, and explore the implication of energetic and kinematic driving of Coulomb explosion of these deuterium containing heteroclusters on NFDCE.

II. VERTICAL IONIZATION OF HETEROCLUSTERS

The multielectron ionization of both homonuclear and heteronuclear clusters is vertical if realized for a fixed atomic geometry of the neutral state. For CVI, Coulomb explosion is described as an expansion of ions with fixed charges in the absence of electrons, which significantly simplifies the simulation of this process.[35,42] When CVI conditions are fulfilled and the initially (prior to ionization) uniform ion density ρ_{mol} remains uniform during the cluster expansion, the dynamics and energetics of Coulomb explosion can be described by analytical equations.[21,28,35,42] Such uniform expansion takes place in a molecular cluster with identical charges q_{mol} on each molecule and an identical q_j/m_j ratio between atomic charges q_j and masses m_j for different j atoms. The last condition implies that the kinematic parameter[20,21,28]

$$\eta = q_j m_{j'}/q_{j'} m_j \tag{1}$$

(with $m_{j'} > m_j$) is $\eta = 1$ for all pairs of ions and that consequently the acceleration of atoms does not depend on their charge and mass.[20,21] To such a class of uniformly expanding clusters belong homonuclear clusters with identical atomic charges and heteronuclear clusters with the kinematic parameter $\eta = 1$, Eq. (1), e.g., $(C^{6+}D_4^+)_n$, $(C^{4+}T_4^+)_n$,[28] or $(O^{8+}D_2^+)_n$.[21]

The dynamics of the ion expansion of the uniformly expanding heteroclusters (Appendix A) was found by modifying the corresponding equation for homonuclear clusters (Paper III). The Coulomb explosion time t of the jth ion located at the initial distance $r_j(0)$ from the cluster center and located at the distance $r_j(t)$ at the time t is given by

$$t = \int_{r_j(0)}^{r_j(t)} dr' \{2E_j[r'; r_j(0)]/m_j\}^{1/2}, \tag{2}$$

where $E_j[r'; r_j(0)]$ is the kinetic energy of a jth type ion, which is moved from $r_j(0)$ to r'. The kinetic energy of a j ion in a uniform expansion can be represented on the basis of simple electrostatic arguments (Appendix A) in the form

$$E_j[r'; r_j(0)] = (4\pi/3)\bar{B}\rho_{\mathrm{mol}} q_{\mathrm{mol}} q_j r_j(0)^2 [1 - r_j(0)/r'], \tag{3}$$

where $\bar{B} = 14.385\,\mathrm{eV\,\AA^{-1}}$, q_{mol} is the molecular-ion charge, and ρ_{mol} is the initial molecular ion density $\rho_{\mathrm{mol}} = (4\pi r_a^3 f/3)^{-1}$, with r_a being the intermolecular spacing within the neutral cluster and f being a packing fraction. m_j

TABLE I. The cluster radius doubling time, Eq. (5), for homonuclear deuterium clusters and methane and water heteroclusters, with uniformly expanding ions ($\eta=1$).

Cluster	D_n	$(C^{6+}D_4^+)_n$	$(C^{4+}T_4^+)_n$	$(O^{8+}D_2^+)_n$
τ_2 (fs)	13.5	7.6	10.3	5.1

and q_j are the atomic mass and the charge of the jth ion (with $m_j/q_j=$const for all j). From Eqs. (2) and (3) the Coulomb explosion time is

$$t=C(m_j/q_{\rm mol}\rho_{\rm mol}q_j)^{1/2}Z(\xi), \tag{4}$$

$$\xi=r_j(0)/r_j(t), \tag{4a}$$

$$Z(\xi)=\frac{(1-\xi)^{1/2}}{\xi}+\frac{1}{2}\ln\left(\frac{1+(1-\xi)^{1/2}}{1-(1-\xi)^{1/2}}\right). \tag{4b}$$

The following units are used herein: m in amu, q in electrons, $r_j(t)$ in angstrom, r_a in angstrom, $\rho_{\rm mol}$ in Å^{-3}, and t in fs. The coefficient C of Eq. (4) is then $C=0.931\ \text{fs Å}^{-3/2}$. Each j ion, initially located at $r_j(0)$, moves at time t to $r_j[t;r_j(0)]$, which, according to Eq. (4) (with $m_j/q_j=$const), is independent of j. Then $r_j[t;r_j(0)]=r_j(0)\xi(t)^{-1}$, so the radial expansion is uniform for all the $\{j\}$ ions. The characteristic Coulomb explosion time $\tau=t(\xi^{-1})$ for the expansion of the cluster radius from its initial value of R_0 by a numerical factor of $\xi^{-1}(>1)$ is given by Eq. (4). The time $\tau_2=t(2)$ for the cluster radius doubling [$\xi^{-1}=2$, $\xi=0.5$, $Z(\xi)=2.296$] is

$$\tau_2=2.137(m_j/q_{\rm mol}q_j\rho_{\rm mol})^{1/2}. \tag{5}$$

The τ_2 data discussed in Appendix B and shown in Table I do not depend on the cluster radius and on the atomic index j. In particular, it should be noted that the τ_2 data for uniformly expanding heteroclusters (presented in Table I) are identical for different ionic species in the same cluster (i.e., C^{6+} and D^+ from $C^{6+}D_4^+$ and C^{4+} and T^+ from $C^{4+}T_4^+$).

We now turn to the energetics of ions from uniformly Coulomb exploding clusters. On the basis of simple electrostatic arguments the kinetic energy $E_j[r(t)]$ of the jth ion, which is located at distance $r(t)$ from the cluster center at time t, is given by Eq. (3). The final ($r'\to\infty$) kinetic energy E_j of the jth ion is

$$E_j[r_j(0)]=(4\pi/3)\bar{B}\rho_{\rm mol}q_{\rm mol}q_jr_j(0)^2, \tag{6}$$

being proportional to the square of its initial distance $r_j(0)$ from the cluster center. A numerical solution of Eq. (4) results in $r_j(t)$, which is substituted into Eq. (3) to find the time dependence of an ion kinetic energy and velocity. By using Eq. (6), the average energy $E_{j,\rm av}$ and the maximal energy $E_{j,\rm M}$ of the ions are given by

$$E_{j,\rm av}=(4\pi/5)\bar{B}\rho_{\rm mol}q_{\rm mol}q_jR_0^2, \tag{7}$$

$$E_{j,\rm M}=(4\pi/3)\bar{B}\rho_{\rm mol}q_{\rm mol}q_jR_0^2, \tag{8}$$

where R_0 is the initial cluster radius. The energy distribution $P(E_j)$ of the j-type ions is

$$P(E_j)=\tfrac{3}{2}(E_j/E_{j,\rm M}^3)^{1/2};\quad E_j\leqslant E_{j,\rm M}. \tag{9}$$

The energetics of Coulomb explosion, Eqs. (6)–(8), which is discussed in Appendix B, is expected to be applicable for uniformly expanding molecular heteroclusters containing several distinct $\{j\}$ ions. From the analysis (Appendix B) of uniform heterocluster expansion, we expect the cluster size dependence to be $E_{j,\rm M}$, $E_{j,\rm av}\propto R_0^2$, the specific ion charge dependence to be $E_{j,\rm M}$, $E_{j,\rm av}\propto q_j$, and $E_{j,\rm M}$, $E_{j,\rm av}\propto q_{\rm mol}$. The number of $E_{j,\rm M}$ values is equal to the number of distinct ions. Finally, the distinct ion energy distributions $P(E_j)\propto E_j^{1/2}$ are manifested in the Coulomb explosion.

The analytical results for Coulomb explosion lifetimes and energies, Eqs. (4) and (7)–(9), provide benchmark reference data, which can be used to define the domain of the heterocluster size and of the laser parameters, where the CVI conditions for uniformly exploding clusters are applicable. The uniform explosion conditions are violated for the common case of $\eta\neq1$. Thus for $(C^{4+}D_4^+)_n$ ($\eta=1.5$), $(C^{4+}H_4^+)_n$ ($\eta=3$), $(O^{8+}T_4^+)_2$ ($\eta=0.67$), and $(O^{8+}H_2^+)_n$ ($\eta=2$) heteroclusters, the analytical relations presented above are inapplicable. The dynamics will then exhibit ion-specific values of τ_2, which become dependent on the cluster size,[21,28] and the energetics will show deviations from Eqs. (6)–(9) even at high intensities when outer ionization is nearly complete. In general, the CVI approximation breaks down at low laser intensities. Under these circumstances we expect inner/outer ionization processes to occur on a slower time scale than at the higher intensities (Paper II), with the outer ionization process being incomplete (Papers I and II). This causes screening effects of the Coulomb repulsions by the nanoplasma electrons, retarding the energetics of Coulomb explosion. These interesting effects of the violation of the CVI model for Coulomb explosion of $(C^{q+}D_4^+)_n$ and of $(C^{q+}H_4^+)_n$ $(q=3-6)$ heteroclusters will be explored by molecular dynamics simulations of the electron dynamics and of nuclear dynamics, using the computational schemes previously advanced by us (Paper I). The heteroclusters were coupled to a Gaussian laser field with a pulse width of $\tau=25$ fs and a peak intensity of $|eF_{\rm M}|=(2.7\times10^{-7})I^{1/2}\ \text{eV Å}^{-1}$ in the intensity range $I=10^{16}-10^{19}\ \text{W cm}^{-2}$. The temporal onset of the Gaussian pulse was taken at $t=t_s<0$, with the intensity dependent t_s values being given in Paper I.

III. KINEMATIC AND ELECTRON DYNAMICS EFFECTS ON COULOMB EXPLOSION OF METHANE HETEROCLUSTERS

Important features of Coulomb explosion of heteroclusters involve the effects of nonuniform nuclear dynamics due to kinematic effects. When $\eta>1$ an overrun effect of the light ions relative to the heavy ions will be manifested in a bimodal energy distribution of the two types of ions. These effects are exhibited in Coulomb explosion of $(C^{q_c+}D_4^+)_n$ and $(C^{q_c+}H_4^+)_n$ ionic heteroclusters (with $q_C=3-6$) in ultraintense laser fields ($I=10^{16}-10^{19}\ \text{W cm}^{-2}$), whose inner/outer electron dynamics induced by Gaussian pulses was already explored by us (Papers I and II). In $(CD_4)_{1061}$ clusters at the lower intensity of $I=10^{16}\ \text{W cm}^{-2}$ the inner ionization saturation level (per molecule) of $n_{\rm ii}=7.7$ (with $q_C=3.7$) is accomplished at the characteristic time of $\tau_{\rm ii}\simeq9$ fs, while the outer ionization saturation level of $n_{\rm oi}=5.1$ is reached at the

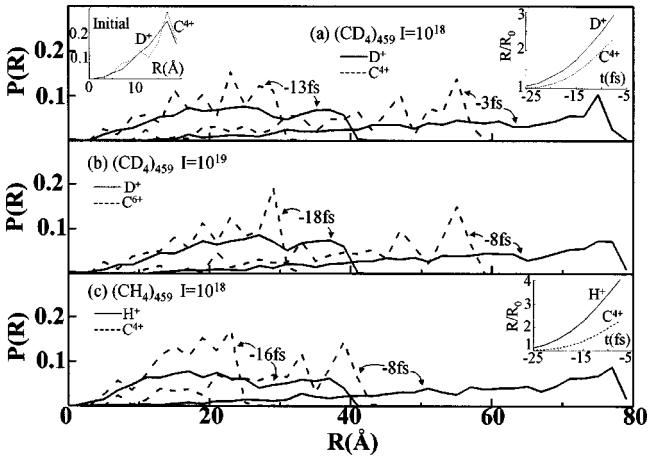

FIG. 1. Coulomb explosion of $(CD_4)_{459}$ heteroclusters at $I=10^{18}\,W\,cm^{-2}$, with the formation of $(C^{4+}D_4^+)_{459}$ (a), of $(CD_4)_{459}$ heteroclusters at $I=10^{19}\,W\,cm^{-2}$, with the formation of $(C^{6+}D_4^+)_{459}$ (b), and of $(CH_4)_{459}$ heteroclusters at $I=10^{18}\,W\,cm^{-2}$, with the formation of $(C^{4+}H_4^+)_{459}$ (c). The laser pulse width is $\tau=25$ fs. The radial distributions $P(R)$ of the light D^+ or H^+ ions (solid curves) and of the heavy C^{q_c+} ions (dashed curves) are shown at different times. The initial times for the onset of the Gaussian laser pulse (Paper I) are $t_s=-30$ fs for $I=10^{18}\,W\,cm^{-2}$ and $t_s=-36$ fs for $I=10^{19}\,W\,cm^{-2}$. The left-hand side inset in (a) shows the initial radial distributions of the D^+ and C^{4+} ions at $t=t_s$. The right-hand side insets to (a) and (c) show the time dependence of the ratios of the radii $R(t)$ of the subclusters, at time t, normalized to the initial cluster radius. (a)–(c) exhibit nonuniform Coulomb explosion, with kinematic overrun effects (see text).

characteristic time of $\tau_{oi}\sim 15$ fs, with a population of residual nanoplasma electrons at $n_p\sim 2.6$. Increasing the laser intensity to $I=10^{18}\,W\,cm^{-2}$ results in $n_{ii}=8$ (with $q_C=4$) at $\tau_{ii}\sim 4$ fs and $n_{oi}=8$ at $\tau_{oi}\sim 4.4$ fs, with a complete depletion of the nanoplasma electrons ($n_p=0$). Finally, even at a higher intensity of $I=10^{19}\,W\,cm^{-2}$ a two-step temporal multielectron inner ionization process is exhibited with $n_{ii}=8$ ($q_C=4$) at $\tau_{ii}=2.8$ fs, increasing to $n_{ii}=10$ ($q_C=6$) at $\tau_{ii}=4.0$ fs, while the outer ionization process saturates for $n_{oi}=10$ with a complete nanoplasma depletion ($n_p=0$), resulting in nuclear $(C^{6+}D_4^+)_n$ cluster matter at $\tau_{oi}\sim 4$ fs. The multielectron ionization and electron dynamics trigger Coulomb explosion.

The Coulomb explosion nuclear dynamics of $(CD_4)_n$ clusters, occurring in parallel to and sequentially with the electron dynamics, is affected by kinematic effects, which trigger a nonuniform ion explosion. The character of this nonuniform explosion is determined by the kinematic parameter, Eq. (1), $\eta=q_D m_C/q_C m_D$. At the laser intensity range $I=10^{16}-10^{18}\,W\,cm^{-2}$, the final charge of the C atom is nearly $q_C=4$, so that $\eta=1.5$. The kinematic parameter $\eta>1$ ensures higher velocities of the light D^+ ions relative to the heavy C^{q_c+} ions, which are initially located at the same distance from the cluster center[28] [Fig. 1(a)]. Due to such a difference in the velocities there is an overrun effect of the D^+ ions relative to the C^{q_c+} ions [Fig. 1(a)]. In the course of the ionized cluster Coulomb explosion, the deuterium D^+ ions and the carbon C^{4+} ions form two expanding subclusters, whose spatial overlap decreases at longer times [Fig. 1(a)]. The time dependence of the subcluster radii R_D and R_C of the D^+ and C^{4+} ions, respectively (defined as the maximal distances of the respective ions from the cluster center), is portrayed in the right-hand side inset to Fig. 1(a), demonstrating the overrun effect of the light ions relative to the heavy ions, with the formation of two distinct, expanding subclusters.

At the laser intensity of $I=10^{19}\,W\,cm^{-2}$ the carbon atoms in the $(CD_4)_n$ clusters are deprived of all their electrons, with the formation of C^{6+} nuclei. This $q_C=6$ charge provides a kinematic parameter, Eq. (1), of $\eta=1$, which indicates a uniform expansion under CVI initial conditions (Appendix A). However, according to our simulations for $I=10^{19}\,W\,cm^{-2}$ [Fig. 1(b)], the expansion is also nonuniform, although somewhat less pronounced than for $I=10^{18}\,W\,cm^{-2}$ [Fig. 1(a)]. The nonuniform ion expansion at $I=10^{19}\,W\,cm^{-2}$ is rationalized by the relatively long time for the extreme outer ionization with the formation of C^{6+} [i.e., $t_{ii}-t_{oi}\simeq 30$ fs (Paper II)], so that a lower value of $q_C\approx 4$ with $\eta\simeq 1.5$ is attained during the time scales of $t-t_s=12$ fs ($t=-18$ fs) and $t-t_s=22$ fs ($t=-8$ fs), which are presented in Fig. 1(b) at $I=10^{19}\,W\,cm^{-2}$. The competition between $C^{4+}\rightarrow C^{6+}$ inner/outer ionization dynamics for $I=10^{19}\,W\,cm^{-2}$ occurs on a time scale which is longer than the characteristic Coulomb explosion times for the two D^+ and C^{4+} ($q=4$) distinct subclusters manifested in Fig. 1(b). Only at longer times (for C^{6+}), i.e., $t-t_s\geqslant t_{ii}-t_{oi}\simeq 30$ fs (or $t\geqslant -5$ fs for the Gaussian pulse), uniform expansion will be manifested. Thus the nonuniform expansion at $I=10^{19}\,W\,cm^{-2}$ is rationalized by the competition between (inner) ionization dynamics and nuclear dynamics.

A marked difference between the expansion of light and heavy ions in Coulomb exploding methane clusters is manifested by $(CH_4)_n$ clusters at $I=10^{18}\,W\,cm^{-2}$ [Fig. 1(c)]. The kinematic parameter for $(C^{4+}H_4^+)_n$ clusters is large, i.e., $\eta=3$. In this case, the difference between the expansion of the light H^+ and the heavy C^{4+} ions is very strongly exhibited, and in the progress of the expansion [i.e., $t\geqslant -8$ fs in Fig. 1(c)] the light H^+ ions form an outer subcluster, which is nearly completely separated from the inner heavy ion C^{4+} subcluster.

Within the course of Coulomb explosion of these methane heteroclusters (Fig. 1), the light H^+ or D^+ ions tend to assemble mainly at the upper edge of their spatial distribution. This situation bears an analogy to the case of Coulomb explosion of spatially, initially inhomogeneous homonuclear clusters with a decreasing density profile towards the cluster boundary.[40] It was proposed that such initially inhomogeneous clusters can even generate shock waves.[40] However, in the case of inhomogeneous Coulomb explosion of the methane heteroclusters explored herein, the compression of the light ions is not detected and these ions cannot generate shock wave phenomena.

IV. ENERGETICS OF COULOMB EXPLOSION OF DEUTERATED METHANE HETEROCLUSTERS

The average energies of the D^+ ions from Coulomb explosion of $(CD_4)_n$ ($n=55-4213$) clusters, which are induced by ultraintense laser fields in the range of $I=10^{17}-10^{19}\,W\,cm^{-2}$, obey the CVI dependence of Eq. (7), $E_{av}\propto R_0^2$ (Fig. 2). However, the slopes of this scaling law

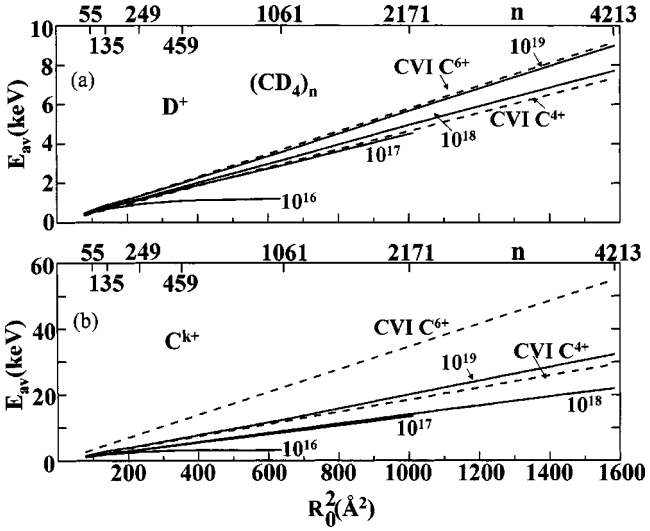

FIG. 2. Cluster size dependence of the average D^+ ion energies (a) and of the average C^{k+} ion energies (b) from $(CD_4)_n$ ($n=55-4213$) induced by Gaussian pulses in the intensity range $I=10^{16}-10^{19}\,\mathrm{W\,cm^{-2}}$ (the numbers 10^x, $x=16-19$, on the curves mark the intensities in units of $\mathrm{W\,cm^{-2}}$). The solid lines represent the simulation results for the average energies vs R_0^2. The results of the CVI approximation, Eq. (7), are presented by dashed lines, calculated for C^{4+} (marked CVI C^{4+}) and for C^{6+} (marked CVI C^{6+}).

exhibit a marked intensity dependence. The intensity dependence of the D^+ ion energies reveals a marked increase in the slope of E_{av} vs R_0^2 from the intensity range of $I=10^{18}\,\mathrm{W\,cm^{-2}}$ to the higher range of $I=10^{19}\,\mathrm{W\,cm^{-2}}$. This effect originates from the intensity dependence of the ionization level of the C atom, which acts as an energetic trigger for the D^+ ions. As, according to Eq. (7), $E_{\mathrm{av}}\propto q_{\mathrm{mol}}(q_{\mathrm{C}}+4q_{\mathrm{D}})$, we expect that $E_{\mathrm{D,av}}$ increases with increasing the ionization level of the cation. At the highest intensity domain of $I=10^{19}\,\mathrm{W\,cm^{-2}}$, C^{6+} nuclei are generated, while in the intensity domain of $I=10^{17}-10^{18}\,\mathrm{W\,cm^{-2}}$ C^{4+} ions are predominantly produced. The ratio κ of the slopes of the simulated $E_{\mathrm{D,av}}\propto R_0^2$ relations for the expansion of D^+ ions from $(C^{6+}D_4^+)_n$ and from $(C^{4+}D_4^+)_n$ is $\kappa=1.17$ (Fig. 2), while the CVI prediction, Eq. (7), is $\kappa=1.25$. As apparent from Fig. 2, the simulation results for the D^+ energetics for $I=10^{19}\,\mathrm{W\,cm^{-2}}$ practically coincide with the CVI scheme, Eq. (7), for C^{6+} (Fig. 2), while the simulation results for $I=10^{18}\,\mathrm{W\,cm^{-2}}$ are slightly higher (by 5%) than the CVI energy, Eq. (7), for C^{4+}. These small positive deviations from the CVI scheme in the high intensity range ($I=10^{18}\,\mathrm{W\,cm^{-2}}$) can be attributed to the overrun effect of the D^+ ions relative to the C^{4+} ions. This analysis, based on the CVI scheme at the highest intensities ($I=10^{18}-10^{19}\,\mathrm{W\,cm^{-2}}$), provides a quantification of the energetic triggering effect, which is slightly affected by the overrun effect for the light ions due to the enhancement of the heavy ion charge. Moving to somewhat lower intensities ($I=10^{16}-10^{17}\,\mathrm{W\,cm^{-2}}$), some slight increase (by $\sim$10%) of the slope of $E_{\mathrm{D,av}}$ vs R_0^2 for D^+ ions between $I=10^{18}\,\mathrm{W\,cm^{-2}}$ and $I=10^{19}\,\mathrm{W\,cm^{-2}}$ is manifested (Fig. 2). Furthermore, at the intensity of $I=10^{17}\,\mathrm{W\,cm^{-2}}$ some weak deviation from the linear $E_{\mathrm{D,av}}\propto R_0^2$ dependence is observed [Fig. 2(a)]. This deviation is due to the screening effects by the nanoplasma, which are minor at this intensity for smaller clusters ($R_0<25$ Å) but become more pronounced for larger clusters. At the lower intensity of $I=10^{16}\,\mathrm{W\,cm^{-2}}$, the CVI $E_{\mathrm{D,av}}\propto R_0^2$ relation only holds for small clusters, $R_0<(R_0)_I\approx 10$ Å, with a cluster size of $n<(n)_I\simeq 55$ Å, where $(R_0)_I$ is the intensity dependent boundary radius for the applicability of the CVI (Paper III), which will be discussed in Sec. V. In the lower intensity domain of $I=10^{16}\,\mathrm{W\,cm^{-2}}$, $E_{\mathrm{D,av}}$ saturates above $R_0>(R_0)_I$, manifesting the persistence of the "long-lived" nanoplasma in larger clusters. This pattern of the size dependence of the D^+ energetics in the Coulomb explosion of $(CD_4)_n$ heteroclusters at $I=10^{16}\,\mathrm{W\,cm^{-2}}$ is qualitatively similar to that of $(D_2)_n$ clusters at $I\simeq 10^{15}\,\mathrm{W\,cm^{-2}}$ (Paper III).

From the simulation results for the energetics of D^+ ions in the Coulomb explosion of $(C^{q_c+}D_4^+)_n$ heteroclusters we infer that the following.

(1) The CVI scaling law, Eqs. (7) and (8), was derived for uniform Coulomb explosion. However, its applicability range is wider.

(2) Energetic triggering: In the higher intensity range ($I=10^{17}-10^{19}\,\mathrm{W\,cm^{-2}}$), general adherence to the CVI size dependence $E_{\mathrm{av}}\propto aR_0^2$ is exhibited, with the slope a of the scaling law being dependent on the ionization level q_{C} of the C atom ($q_{\mathrm{C}}=4$ at $I\simeq 10^{17}-10^{18}\,\mathrm{W\,cm^{-2}}$ and $q_{\mathrm{C}}=6$ at $I=10^{19}\,\mathrm{W\,cm^{-2}}$), and also on kinematic overrun effects [point (4)] and on Gaussian pulse shape effects [point (5)].

(3) Screening by the nanoplasma: In the lower intensity range ($I=10^{16}-10^{17}\,\mathrm{W\,cm^{-2}}$) nanoplama screening effects result in a marked deviation from the CVI size dependence.

(4) Nonuniform explosion: For nonuniformly expanding nanoclusters in the high intensity domain, kinematic overrun effects of the light D^+ ions relative to the heavy C^{q_c+} ions are expected to result in the increase of the slope a of the scaling law relative to that expected for uniformly exploding clusters, as exhibited at $I=10^{18}\,\mathrm{W\,cm^{-2}}$.

(5) Uniform explosion: The nearly perfect agreement between the CVI relation with $q_{\mathrm{C}}=6$ for uniform Coulomb explosion and the simulation results for the explosion of $(C^{6+}D_4^+)_n$ clusters ($\eta=1$) at $I=10^{19}\,\mathrm{W\,cm^{-2}}$ reflects on the near attainment of the uniform Coulomb explosion of heteroclusters. Negative deviations of the energetics from the CVI relation (for $q_{\mathrm{C}}=6$), due to the early formation of C^{4+} and pseudo-CVI effects [point (6)], seem to be small.

(6) Pseudo-CVI domain: For clusters driven by a Gaussian laser pulse, adiabatic following of the Coulomb explosion is expected to result in some retardation of the slope a of the scaling law, even for the highest intensities. The difference between the CVI relation for uniform explosion and the simulation results for the nonuniform explosion of $(C^{4+}D_4^+)_n$ clusters at $I=10^{18}\,\mathrm{W\,cm^{-2}}$ presumably originates from cancellation of the contributions of kinematic overrun effect, which enhances slope a, and the pseudo-CVI driving, which reduces a, with the former effect being dominating.

The energetics of the C^{q_c+} ions ($q_{\mathrm{C}}\simeq 4$ at $10^{17}-10^{18}\,\mathrm{W\,cm^{-2}}$ and $q_{\mathrm{C}}=6$ at $I=10^{19}\,\mathrm{W\,cm^{-2}}$) exhibits a linear $E_{\mathrm{C,av}}$ versus R_0^2 dependence (Fig. 2), as inferred from the CVI, Eq. (7). However, quite marked deviations of the

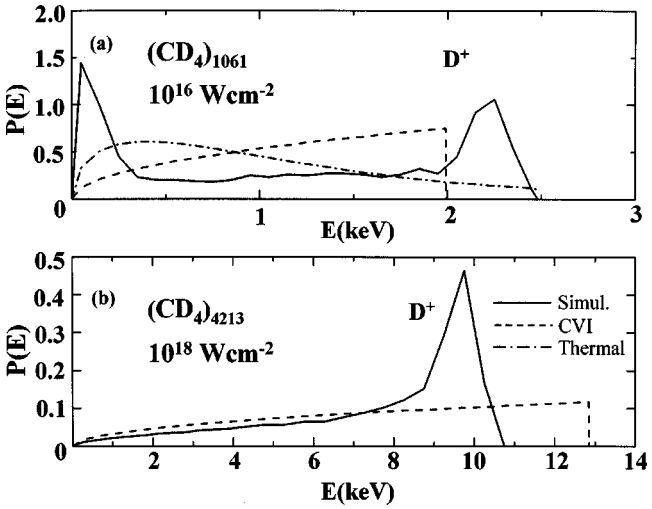

FIG. 3. Energy distributions of D^+ ions from Coulomb explosion of $(CD_4)_n$ ($n=1061$ and 4213) heteroclusters induced by Gaussian laser pulses at $I=10^{16}\,\mathrm{W\,cm^{-2}}$ (a) and at $I=10^{18}\,\mathrm{W\,cm^{-2}}$ (b). The simulated results (——) are compared with the CVI for uniform explosion (----) and with the thermal distribution (-·-·-). The simulation results at $I=10^{18}\,\mathrm{W\,cm^{-2}}$ show a marked deviation from the CVI for uniform explosion, Eq. (9), due to kinematic overrun effects, while the simulation results at $I=10^{16}\,\mathrm{W\,cm^{-2}}$ manifest a bimodal distribution.

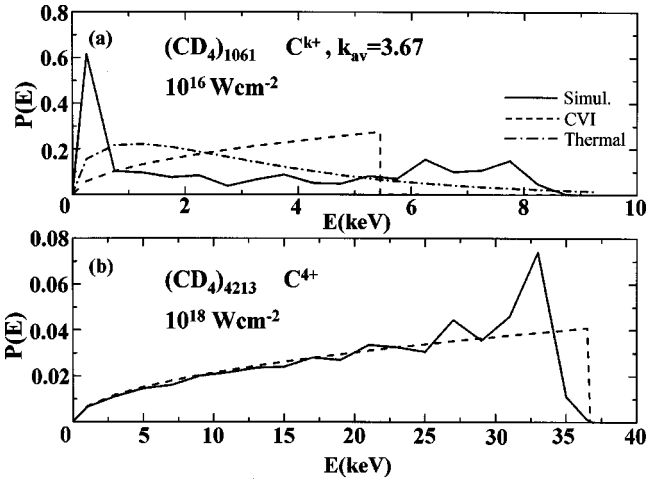

FIG. 4. Energy distribution of C^{k+} ions from Coulomb explosion of $(CD_4)_n$ ($n=1061$ and 4213) heteroclusters induced by a Gaussian laser pulse at $I=10^{16}\,\mathrm{W\,cm^{-2}}$ (a) and at $I=10^{18}\,\mathrm{W\,cm^{-2}}$ (b). The simulated results (——) are compared with the CVI for uniform explosion (----) and with the thermal distribution (-·-·-). The simulation results at $I=10^{18}\,\mathrm{W\,cm^{-2}}$ are in reasonable agreement with the CVI for uniform explosion, Eq. (9), manifesting the uniform expansion of the $(C^{4+})_{4213}$ subcluster. The simulation results at $I=10^{16}\,\mathrm{W\,cm^{-2}}$ can neither be fitted by the CVI nor by the thermal distributions.

$E_{\mathrm{C,av}}$ simulation data from the CVI predictions, Eq. (7), are exhibited, with the simulation data for C^{4+} and for C^{6+} being lower by ~32% and by ~42%, respectively, from the corresponding CVI predictions [Fig. 2(b)]. These deviations are due to two effects, which for the heavy ions operate in the same direction: (a) kinematic effects for the heavy ions, which are left behind, being overrun by the light ions, and (b) laser pulse shape effects manifested for Gaussian pulses in the pseudo-CVI domain. The enhancement $\kappa_{\mathrm{C,D}}$ of the C^{q_c+} heavy ion energies relative to the D^+ energies from the simulation results [Figs. 2(a) and 2(b)] are $\kappa_{\mathrm{C,D}}=2.8$ for $q_{\mathrm{C}}=4$ at $I=10^{18}\,\mathrm{W\,cm^{-2}}$ and $\kappa_{\mathrm{C,D}}=3.6$ for $q_{\mathrm{C}}=6$ at $I=10^{19}\,\mathrm{W\,cm^{-2}}$. From the CVI relations for uniform explosion, Eq. (7), we infer that $\kappa_{\mathrm{C,D}}=q_{\mathrm{C}}/q_{\mathrm{D}}$, so that $\kappa_{\mathrm{C,D}}=4$ for $q_{\mathrm{C}}=4$ and $\kappa_{\mathrm{C,D}}\simeq 6$ for $q_{\mathrm{C}}=6$, which are somewhat higher than the simulation results for the nonuniform case.

The energy distribution of the product ions in Coulomb explosion is presented in Figs. 3 and 4. At the higher laser intensity $I=10^{18}\,\mathrm{W\,cm^{-2}}$, about 75% of the D^+ ions lie in a narrow energy interval, $E=6.5-10.5\,\mathrm{keV}$ [Fig. 3(b)]. This D^+ ion energy distribution shows marked deviations from the uniform cluster expansion $P(E)\propto E^{1/2}$, Eq. (9), with the peak at 9.5 keV and the narrow higher-energy distribution around it being due to kinematic effects, manifesting the overrun of the heavy C^{4+} ions by the light D^+ ions. We previously observed this effect in the explosion of heteroclusters.[21] The signature of the kinetic overrun effects in the nonuniform Coulomb explosion of heteroclusters is manifested by (1) the appearance of a high-energy peak in $P(E)$ for the light ions and (2) the maximal energy being close to the peak and considerably lower than the CVI energy, $E_{\mathrm{D,M}}$, Eq. (8). Accordingly, a representation of energetic data for the light ions in terms of E_{av} instead of the maximal energy should be preferred.

In contrast, the energy distribution of the heavy C^{4+} ions at this high laser intensity [Fig. 4(b)] is broad and similar to that expected for the CVI energy distribution, Eq. (9). The qualitative difference between the energy distributions of the light D^+ ions and the heavy C^{4+} ions at $I=10^{18}\,\mathrm{W\,cm^{-2}}$ reflects on the qualitative differences between the two expanding subclusters, with the heavy C^{4+} ion subcluster reflecting a nearly uniform Coulomb explosion, while the D^+ light ion subcluster manifests kinematic overrun effects.

At the lower laser intensity of $I=10^{16}\,\mathrm{W\,cm^{-2}}$ the D^+ ion distribution is bimodal, revealing both a high-energy component and a low-energy component [Fig. 3(a)]. The peak of the first component lies at a higher energy than the CVI energy maximum, $E_{\mathrm{D,M}}$, Eq. (8), whereas the second component is located at very low energies [Fig. 3(a)]. A similar bimodal energy distribution is also manifested for the C^{k+} ($k=3.7$) ions, where the high energy peak is less pronounced [Fig. 4(a)] than for the D^+ ions [Fig. 3(a)]. This bimodal distribution of the D^+ and C^{k+} ions at $I=10^{16}\,\mathrm{W\,cm^{-2}}$ is unique for Coulomb explosion of heteroclusters, when nanoplasma screening effects prevail. The energy distributions of both types of ions produced by Coulomb explosion of $(CD_4)_n$ heteroclusters at $I=10^{16}\,\mathrm{W\,cm^{-2}}$ [Figs. 3(a) and 4(a)] differ significantly both from those of uniformly exploding clusters, Eq. (9), and from those of the thermal distribution $P(E)\propto(E/E_{\mathrm{av}})^{1/2}\exp(-3E/2E_{\mathrm{av}})$.

V. KINEMATIC EFFECTS MANIFEST ISOTOPE EFFECTS ON THE ENERGETICS OF COULOMB EXPLOSION OF METHANE HETEROCLUSTERS

The CVI relations for the energetics of uniformly exploding clusters, Eqs. (7) and (8), predict the absence of isotope effects on the energetics of the light ions (Appendix

B). However, new facets of isotope effects on the energetics of Coulomb explosion of A^+ light ions from Coulomb explosion of $(C^{4+}A_4^+)_n$ clusters (A=H or D) can originate, in principle, either from electron dynamics or from nuclear dynamics. The electronic contribution was found to be negligibly small, while isotope effects will be dominated by kinematic effects on the nuclear dynamics. The time scales for inner ionization τ_{ii} and for outer ionization τ_{oi} of methane clusters (Paper II) do not exhibit any significant isotope effects in methane heteroclusters. For example, at $I=10^{18}\,\mathrm{W\,cm^{-2}}$, the $(CH_4)_{1061}$ cluster is characterized by $\tau_{ii}=3.7$ fs and $\tau_{oi}=4.3$ fs, as compared to $\tau_{ii}=3.9$ fs and $\tau_{oi}=4.4$ fs for the $(CD_4)_{1061}$ cluster (Table I of Paper II). On the other hand, due to the difference in the kinematic parameters for $(CD_4)_n$ (η=1.5) and for $(CH_4)_n$ (η=3) the isotope effect will be manifested in Coulomb explosion dynamics. From the foregoing discussion (Sec. III), the overrun effect for $\eta>1$ results in a nonuniform expansion and in the enhancement of the (average) energy of the light ions. This enhancement will result in light ion energies which exceed the CVI energy, Eq. (7). The increase in the average energies, relative to the CVI, is moderately small for D^+ from Coulomb explosion of $(C^{4+}D_4^+)_n$ [see data for $I=10^{18}\,\mathrm{W\,cm^{-2}}$ in Fig. 2(a)]. As η provides a measure of the kinematic overrun effects, we expect that the energy increase relative to the CVI energy for uniform explosion will increase with increasing η and will be larger for H^+ ions produced from $(C^{4+}H_4^+)_n$ clusters (η=3) than for D^+ ions produced from $(C^{+4}D_4^+)_n$ heteroclusters (η=1.5). This expectation is confirmed by our simulations (Fig. 5), which show that at $I=10^{18}\,\mathrm{W\,cm^{-2}}$ and at $I=10^{19}\,\mathrm{W\,cm^{-2}}$ the average H^+ energies from $(CH_4)_n$ clusters exceed the average D^+ energies from $(CD_4)_n$ clusters by about $\alpha_{H,D}\simeq 9\%-11\%$. $\alpha_{H,D}$ for a pair of clusters is cluster size independent. $\alpha_{H,D}$ manifests isotope effects due to kinematic overrun effects in a pair of expanding clusters. The isotope effect for the pair $(C^{4+}H_4^+)_n$ (η=3) and $(C^{4+}D_4^+)_n$ (η=1.5) and for the pair $(C^{6+}H_4^+)_n$ (η=2) and $(C^{6+}D_4^+)_n$ (η=1) is nearly identical and reflects on the dependence of $\alpha_{H,D}$ on the ratio of the kinematic parameters for the pair of Coulomb exploding clusters.

In the domain of pseudo-CVI ionization ($I\geqslant 10^{17}\,\mathrm{W\,cm^{-2}}$), the energy distributions of both protons and neutrons exhibit marked deviations from the CVI, with both cases exhibiting a narrow, high-energy peak (Fig. 5). However, the high-energy distribution of the protons is narrower than of the deuterons (Fig. 5). For example, at $I=10^{18}\,\mathrm{W\,cm^{-2}}$, about 76% of the protons produced from $(C^{4+}H_4^+)_{4213}$ clusters are located in the energy range of 8–10 keV, while for deuterons produced from $(C^{4+}D_4^+)_{4213}$ clusters the same fraction of D^+ ions is located in the energy range of 6.5–10.5 keV (Fig. 5 and Sec. IV). Due to the narrower energy distribution of the protons that peak at lower energies (insets to Fig. 5), the maximal energy of the protons is lower than of the deuterons, manifesting an apparent inverse isotope effect. The decrease of the energy distribution width, with increasing the kinematic parameter η, constitutes another feature of the nonuniform Coulomb explosion of size-selected heteroclusters.

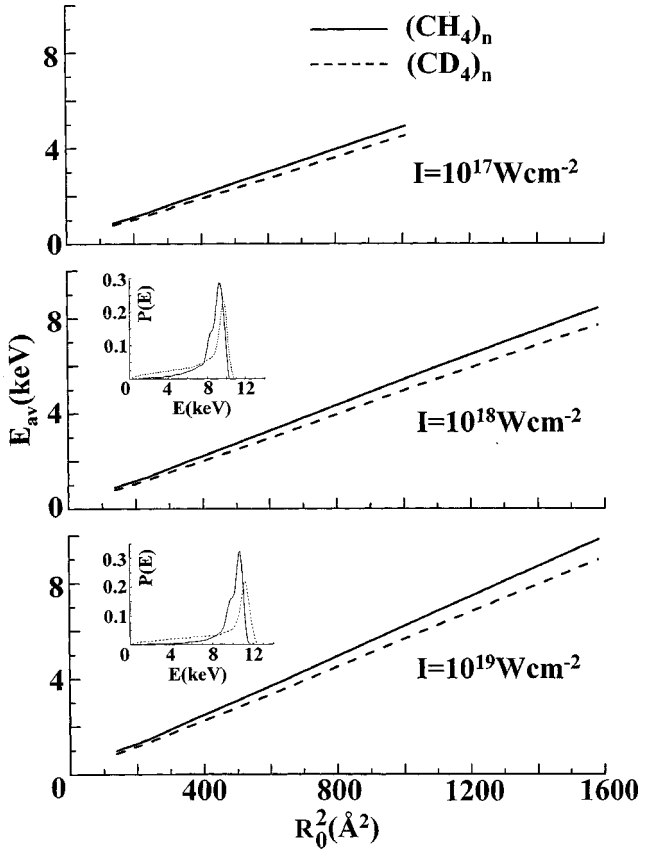

FIG. 5. Isotope effects on the energetics of nonuniform Coulomb explosion of $(CH_4)_n$ and $(CD_4)_n$ heteroclusters ($n=55-4213$). Average energies vs R_0^2 are presented for $(CH_4)_n$ (——) and for $(CD_4)_n$ (----) for $I=10^{17}\,\mathrm{W\,cm^{-2}}$ (upper panel), $I=10^{18}\,\mathrm{W\,cm^{-2}}$ (middle panel), and $I=10^{19}\,\mathrm{W\,cm^{-2}}$ (lower panel). The insets show the energy distributions of the H^+ ions from $(CH_4)_{4213}$ (——) and of the D^+ ions from $(CD_4)_{4213}$ (----) at $I=10^{18}\,\mathrm{W\,cm^{-2}}$ (middle panel) and at $I=10^{19}\,\mathrm{W\,cm^{-2}}$ (lower panel).

VI. BOUNDARY HETEROCLUSTER SIZE FOR THE CVI DOMAIN

Simulations of the energetics of Coulomb explosion of $(CD_4)_n$ clusters induced by a Gaussian pulse (Fig. 2) established the cluster size and the intensity domain for the applicability of the CVI relation (Sec. IV). We have established the applicability range of the CVI size dependence $E_{D,av}\propto R_0^2$ for $R_0<(R_0)_I$, where $(R_0)_I$ is the boundary radius at the intensity I (Sec. IV). For $(CD_4)_n$ heteroclusters the breakdown of the CVI is realized for $(R_0)_I=10$ Å at $I=10^{16}\,\mathrm{W\,cm^{-2}}$ and for $(R_0)_I=31$ Å at $I=10^{17}\,\mathrm{W\,cm^{-2}}$ (Sec. IV). The pattern of the intensity dependence $(R_0)_I\propto I^{1/2}$ of the boundary radius for the energetics of Coulomb exploding $(C^{q_C+}D_4^+)_n$ (q_C=4,6) heteroclusters (Fig. 2) is qualitatively similar to those of $(D^+)_n$ homonuclear clusters (Paper III). From our previous analysis (Paper III) we can relate the dynamics of nuclear Coulomb explosion and of outer ionization electron dynamics of heteroclusters induced by a Gaussian pulse.

The boundary radius $(R_0)_I$ can be inferred from the cluster size which corresponds to complete outer ionization at a given laser intensity. $(R_0)_I$ was obtained from the simulation results for the attainment of the complete outer ionization level $n_{oi}(t)$ (per molecule). Following the procedure of Paper

III, $(R_0)_I$ was taken for complete (taken as 95%) outer ionization, i.e., $n_{oi}(t=0)=0.95$ (taken at the peak of the Gaussian pulse at $t=0$). A theoretical estimate of $(R_0)_I$ rests on the electrostatic model advanced by us. Adopting the formalism developed in Paper III for $(CD_4)_n$ heteroclusters, the outer ionization level is given by

$$n_{oi}(t)=eF_{\ell 0}(t)[R(t)]^2/\sqrt{2}\bar{B}q_{mol}n, \tag{10}$$

where $F_{\ell 0}(t)$ is the laser Gaussian electric field envelope at time t, with the peak $F_{\ell 0}(t)=F_M$. $R(t)$ is the cluster radius at time t, respectively. Following the procedure of Paper III, the boundary radius is then

$$(R_0)_I=eF_M/\sqrt{2}(4\pi/3)\bar{B}\rho_{mol}q_{mol}\xi_0^2, \tag{11}$$

where $\xi_0=R_0/R(t=0)$ is the cluster size expansion parameter. $(R_0)_I$ assumes the numerical value

$$(R_0)_I=3.3\times 10^{-9}I^{1/2}/\rho_{mol}q_{mol}\xi_0^2. \tag{12}$$

with I in W cm^{-2}, ρ_{mol} in Å^{-3}, q_{mol} in electrons, and $(R_0)_I$ in angstroms.

Estimates of $(R_0)_I$, Eq. (12), were performed using $\rho_{mol}=0.016$ Å^{-3}. The cluster size expansion parameter was taken from the fit of the simulation data for $(R_0)_I$ at $I=10^{16}$ W cm^{-2}, which gave $\xi_0=0.45$, and at $I=10^{17}$ W cm^{-2}, which gave $\xi_0=0.40$. The ξ_0 value of $\xi_0=0.4$ was chosen, was assumed to hold for higher intensities as well, and was taken to be independent of the laser intensity. This ξ_0 value for $(CD_4)_n$ heteroclusters was lower than the cluster size expansion parameter $\xi_0=0.55$ for $(D)_n$ clusters (Paper III). In the intensity range of $I=10^{16}-10^{20}$ W cm^{-2}, we accounted for the intensity dependence of the ionization level of the C atom, taking $q_{mol}=q_C+4q_D$, with $q_C=4$ for $I=10^{16}-10^{18}$ W cm^{-2} and $q_C=6$ for $I=10^{19}-10^{20}$ W cm^{-2}. The laser intensity dependence of $(R_0)_I$ (Fig. 6) reflects a break at $I=10^{19}$ W cm^{-2}, due to the enhancement of the inner ionization of C from the C^{4+} ion to the C^{6+} nucleus. At a fixed intensity the value of $(R_0)_I$ is lower for the $(CD_4)_n$ heterocluster than for the $(D)_n$ homonuclear cluster (Fig. 6), in view of the larger value of $\rho_{mol}q_{mol}$ for the heterocluster, according to Eq. (12).

Another result for the characterization of the upper limit of the applicability of the CVI is the average D^+ ion energy $(E_{D,av})_I$ at the boundary $(R_0)_I$, which corresponds to the given intensity I. Using Eq. (12) for $(R_0)_I$ and the CVI energy, Eq. (7), a reasonable approximation for the boundary energy $(E_{D,av})_I$ of the D^+ ion from Coulomb explosion of $(CD_4)_n$ clusters is

$$(E_{D,av})_I=(4\pi/5)\bar{B}\rho_{mol}q_{mol}q_j[(R_0)_I]^2 \tag{13}$$

with $(R_0)_I$ being given by Eq. (12). The average boundary energy is then given by

$$(E_{D,av})_I=3.7\times 10^{-16}q_jI/\rho_{mol}q_{mol}\xi_0^4 \tag{14}$$

with $E_{D,av}$ in eV and I in W cm^{-2}. For a fixed value of $\xi_0=0.4$, the cluster radius $(R_0)_I$, Eq. (12), and the energy $(E_{D,av})_I$ of the D^+ ions ($q_j=1$), Eqs. (12) and (14), become proportional to $I^{1/2}/q_{mol}$ and to I/q_{mol}, respectively,

$$(R_0)_I=\Phi_R I^{1/2}/q_{mol}, \tag{15a}$$

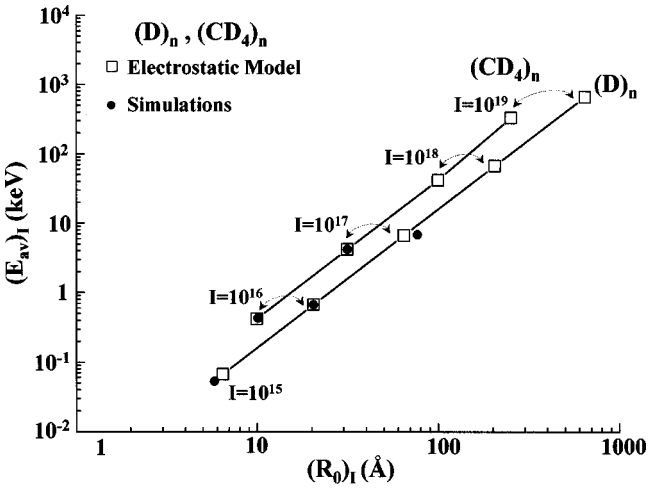

FIG. 6. The relation of the boundary cluster radius $(R_0)_I$ for the applicability of the CVI and the corresponding average D^+ ion energy, $(E_{D,av})_I$, for Coulomb explosion of $(CD_4)_n$ heteroclusters [data marked as $(CD_4)_n$] in the intensity range $I=10^{16}-10^{19}$ W cm^{-2} (the numbers 10^x, $x=15-19$, marking the points, represent intensities in units of W cm^{-2}). The simulation results, marking a complete level (95%) of outer ionization, are represented by black dots. The predictions of the electrostatic model (see text), Eqs. (11)–(15), are represented by open squares. The solid line connects the data of the electrostatic model to guide the eye. Note the positive deviation from the scaling relation at $I=10^{19}$ W cm^{-2} due to the $q_C=4\rightarrow 6$ enhancement of the ionization level of C^{q_c+}. The data of $(R_0)_I$ and of $(E_{av})_I$ for D^+ from Coulomb explosion of $(D)_n$ clusters in the intensity range $I=10^{15}-10^{19}$ W cm^{-2} [marked as $(D)_n$], which were taken from Paper III, are also included.

$$(E_{D,av})_I=\Phi_E I/q_{mol}. \tag{15b}$$

Taking $\rho_{mol}=0.016$ Å^{-3} and $\xi_0=0.4$ results in $\Phi_R=1.25\times 10^{-6}$ Å W$^{-1/2}$ cm and $\Phi_E=9\times 10^{-13}$ eV W^{-1} cm. By fitting the simulation results for $I=10^{17}$ W cm^{-2} [$q_{mol}=8$, $(R_0)_I=31.4$ Å, and $(E_{D,av})_I=4160$ eV], we obtained the corrected coefficients $\Phi_R=8\times 10^{-7}$ Å W$^{-1/2}$ cm and $\Phi_E=3.3\times 10^{-13}$ eV W^{-1} cm^2, which were used for our calculations. In Fig. 6 we present the relation between $(E_{av})_I$ and $(R_0)_I$ for Coulomb explosion of $(CD_4)_n$ clusters obtained from the electrostatic model and from our simulations of the electron outer ionization depletion dynamics. A good agreement between the model and the simulations at $I=10^{16}-10^{17}$ W cm^{-2} is achieved. The $(CD_4)_n$ data (Fig. 6) reveal an upward break in the $(E_{D,av})_I$ versus $(R_0)_I$ dependence at $I=10^{19}$ W cm^{-2} due to the $C^{4+}\rightarrow C^{6+}$ enhancement of the inner ionization at this intensity, which increases the value of $q_{mol}=(q_C+4q_D)$ in Eq. (13) from $q_{mol}=8$ at $I<10^{19}$ W cm^{-2} to $q_{mol}=10$ at $I\geqslant 10^{19}$ W cm^{-2}. This analysis establishes the CVI size domain for the production of energetic D^+ ions from Coulomb explosion of $(CD_4)_n$ heteroclusters. In Fig. 6 we also compare the $(E_{D,av})_I$ versus $(R_0)_I$ relation for Coulomb explosion of $(CD_4)_n$ and the quadratic $(E_{av})_I$ versus $(R_0)_I$ relation for Coulomb explosion of $(D)_n$ clusters (Paper III). As evident from Fig. 6 the $(E_{av})_I$ versus $(R_0)_I$ superquadratic relation for the $(CD_4)_n$ heteroclusters is higher than the quadratic relation for the $(D)_n$ heteroclusters, reflecting on the enhancement of the energetics of the D^+ ion from Coulomb explosion of deuterium containing heteroclusters due to energetic triggering by the

heavy, multicharged ions. This energetic triggering effect in heteroclusters by the C^{q_C+} ions is further increased at $I=10^{19}\,W\,cm^{-2}$ by the increase of q_C (4→6). The energetic triggering of the energetics of the D^+ ion in the Coulomb explosion of deuterium containing heteroclusters is of considerable importance in the context of NFDCE, which will now be addressed.

VII. *dd* NUCLEAR FUSION

Very high average D^+ energies can be generated by Coulomb explosion of $(CD_4)_n$ heteroclusters under realistic CVI conditions (Fig. 6), i.e., $(E_{D,av})_I=4.2\,keV$ at $I=10^{17}\,W\,cm^{-2}$ $[(R_0)_I=31\,Å]$ and $(E_{D,av})_I=42\,keV$ at $I=10^{18}\,W\,cm^{-2}$ $[(R_0)_I\approx 100\,Å]$. Such high deuteron energies from Coulomb explosion of individual heteroclusters can induce effective *dd* nuclear fusion in the (macroscopic) plasma resulting from the outer ionization/Coulomb explosion of a beam of such heteroclusters.[18,19,25,28,29] In what follows we shall provide estimates of the *dd* fusion rate and the neutron generation yields in the macroscopic plasma, following a kinetic scheme previously advanced by us.[28] The outstanding issues pertain to the cluster size dependence and the laser intensity dependence of the *dd* fusion rates and the neutron yields. These *dd* fusion rates and yields for NFDCE of $(CD_4)_n$ heteroclusters will be confronted with the corresponding data for NFDCE of $(D)_n$ homonuclear clusters. We consider D^+ generation via Coulomb explosion of size selected $(CD_4)_n$ clusters. The colliding deuterons can be described as a homogeneous gas of uniformly distributed nuclei and with randomly oriented velocities. The fusion rate in such a gas is[43]

$$R=(1/2)\rho\langle\sigma v\rangle, \tag{16}$$

where ρ is the deuteron density inside the reaction volume V_r, v is the relative velocity of the colliding nuclei, σ is the fusion cross section,[44,45] and the brackets $\langle\ \rangle$ mean the average over the energy distribution of the colliding nuclei.[43] Averaging over the colliding particle energies E_1 and E_2 in the laboratory frame and over the collision angle α, one obtains[28]

$$\langle\sigma v\rangle=\tfrac{1}{2}\int_0^\infty P(E_1)dE_1\int_0^\infty P(E_2)dE_2\int_0^\pi \sigma(E)\times(2E/m_D)^{1/2}\sin\alpha\,d\alpha \tag{17}$$

with the energy distribution $P(E)$ functions normalized to unity. The collision energy E, which is required for the calculation of the fusion cross section, is

$$E=E_1+E_2-2(E_1E_2)^{1/2}\cos\alpha. \tag{18}$$

The *dd* fusion reaction cross section is customarily expressed by the equation[43,45]

$$\sigma(E)=(S/E)\exp(-A/E^{1/2}) \tag{19}$$

with the parameters A and S taken as constants, with $A=45\,keV^{1/2}$ and $S=1.8\times10^{-22}\,keV\,cm^{-2}$.[46] Using the dimensionless variables $x_1=E_1/E_{av}$ and $x_2=E_2/E_{av}$ and the dimensionless parameter

$$X=A/E_{av}^{1/2} \tag{20}$$

one obtains

$$\langle\sigma v\rangle=v_{av}(S/E_{av})G(X), \tag{21}$$

where E_{av} is expressed in keV, v_{av} is the velocity in cm/s of a particle with the kinetic energy E_{av}, $\langle\sigma v\rangle$ is expressed in $cm^3\,s^{-1}$, and $G(X)$ is a reduced function determined only by the energy distribution functions, being given by

$$G(X)=\frac{1}{2}\int_0^\infty P(x_1)dx_1\int_0^\infty P(x_2)dx_2\int_0^\pi x^{-1/2}\times\exp(-Xx^{-1/2})\sin\alpha\,d\alpha. \tag{22}$$

In the case of monoenergetic particles and a large value of X, i.e., $X>5$, the function $G(X)$ is expressed in the analytical form[28]

$$G(X)=(2/X)\exp(-X/2)[1-(3/X)]. \tag{23}$$

A cursory examination of Eqs. (21) and (22) shows that in the case of *dd* NFDCE of deuterium containing clusters, the major contribution to $\langle\sigma v\rangle$ originates from near-front collisions in the high-energy portion of the deuteron distribution. This situation prevails both for $(CD_4)_n$ heteroclusters, where kinematic effects enhance the high energy peak in $P(E)$, and for $(D_2)_n$ homonuclear clusters with $P(E)\propto E^{1/2}$ for $E\leqslant E_M$. The energy distribution of deuterons from Coulomb explosion of both heteroclusters and homonuclear clusters is characterized by an upper cutoff, maximal energy. This situation is in contrast with the thermal distribution for thermonuclear reactions, where the main contribution to the *dd* fusion originates from collisions of deuterons from the high-energy thermal ''tail'' of the distribution with other neutrons.

In the general case of an arbitrary energy distribution, the $G(X)$ function has to be calculated numerically using the simulation data for $P(X)$ [Figs. 3(a) and 3(b)]. The energy distribution of deuterons produced by Coulomb explosion of $(CD_4)_n$ clusters (Fig. 3) reveals that the dominant contribution to $\langle\sigma v\rangle$, Eqs. (21) and (22), originates from the high-energy region, where $P(X)$ can be approximated by a Gaussian function. Accordingly the deuteron energy distribution of deuterons from $(CD_4)_n$ clusters was approximately described by the Gaussian function

$$P(E)=\frac{\gamma}{\theta E_{av}\sqrt{\pi}}\exp\left[-\left(\frac{E-\epsilon E_{av}}{\theta E_{av}}\right)^2\right], \tag{24}$$

where γ stands for the fraction of ions whose energy lies inside the Gaussian [with $P(E)$ in Eq. (24) being normalized to γ], $E_c=\epsilon E_{av}$ is the Gaussian center, and θE_{av} is the Gaussian width. The $G(X)$ function for the arbitrary Gaussian of Eq. (24) is readily expressed in terms of the G function for the standard Gaussian with $\gamma=\epsilon=1$ by the scaling relation

$$G_{\gamma,\epsilon,\theta}(X)=\gamma^2\epsilon^{-1/2}G_{1,1,\tilde{\theta}}(\tilde{X}), \tag{25}$$

where

$$\tilde{\theta}=\theta/\epsilon,\quad \tilde{X}=X\epsilon^{-1/2}. \tag{26}$$

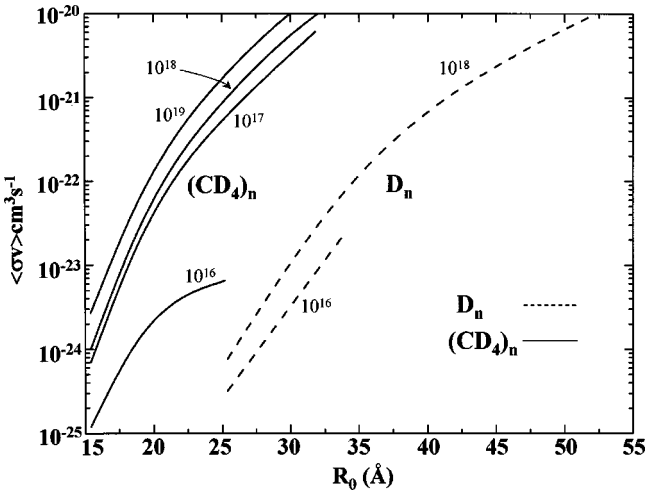

FIG. 7. The kinetic parameters $\langle \sigma v \rangle$ averaged over the energy distribution of colliding deuterons for the *dd* nuclear fusion for NFDCE of $(CD_4)_n$ ($n=55-4213$) heteroclusters (——) and of $(D)_n$ ($n=55-33573$) homonuclear clusters (----) in the intensity range $10^{16}-10^{19}\,W\,cm^{-2}$. The numbers 10^x, $x=16-19$, on the curves mark the intensities in unity of $W\,cm^{-2}$. The $\langle \sigma v \rangle$ data were calculated from Eqs. (21), (22), and (24) (see text).

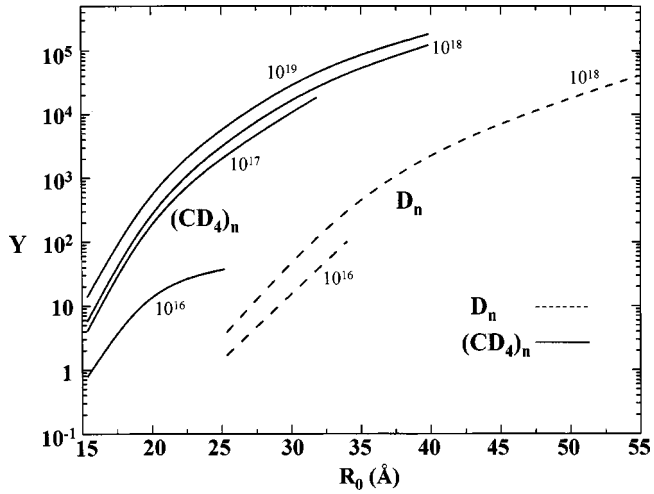

FIG. 8. Neutron yields per laser pulse for *dd* NFDCE of $(CD_4)_n$ ($n=55-4213$) heteroclusters (——) and for $(D)_n$ ($n=55-33573$) homonuclear clusters (----) in the intensity range $I=10^{16}-10^{19}\,W\,cm^{-2}$. The numbers 10^x, $x=16-19$, on the curves, mark the intensities in units of $W\,cm^{-2}$. The neutron yields were calculated from Eq. (27) together with the data of Fig. 7, using the experimental conditions of the Lawrence-Livermore experiment (Ref. 13).

Using the average energies E_{av} obtained from the simulation for $(CD_4)_n$ clusters (Fig. 2), we calculated from Eqs. (21) and (24)–(26) the $\langle \sigma v \rangle$ values for NFDCE of the $(CD_4)_n$ clusters (Fig. 7). We also calculated by numerical integration of Eq. (22) the $\langle \sigma v \rangle$ values for the NFDCE of deuterium $(D)_n$ clusters where the deuteron energy distribution (Paper III) is described in terms of the function $P(E) \propto (E/E_M)^{1/2}$, Eq. (9). The $\langle \sigma v \rangle$ data for the NFDCE of $(CD_4)_n$ and $(D)_n$ clusters (Fig. 7) manifest marked laser intensity dependence and cluster size dependence. For each I, $\langle \sigma v \rangle$ increased with increasing R_0. For $(CD_4)_n$ clusters at the lower intensity of $I=10^{16}\,W\,cm^{-2}$, the $\langle \sigma v \rangle$ data exhibit a weaker increase with increasing R_0 than in the higher intensity range of $I=10^{17}-10^{19}\,W\,cm^{-2}$, due to nanoplasma screening effects. In the higher intensity range $I=10^{18}-10^{19}\,W\,cm^{-2}$, the size dependence $\langle \sigma v \rangle$ is qualitatively similar; however, for a fixed value of R_0 the $\langle \sigma v \rangle$ values are higher for $I=10^{19}\,W\,cm^{-2}$ (where $q_C=6$) than for $I=10^{18}\,W\,cm^{-2}$ (where $q_C=4$) due to the enhancement of energetic triggering effects at the higher intensity. The size dependence of $\langle \sigma v \rangle$ at high intensities for both $(CD_4)_n$ and $(D)_n$ clusters manifests the empirical size relation $\langle \sigma v \rangle = \bar{\alpha} \exp(-\beta/R_0)$, where $\bar{\alpha}$ and β depend on the nature of the cluster and on I, with $\beta=270$ Å for $(CD_4)_n$ at $I \geqslant 10^{17}\,W\,cm^{-2}$ and $\beta=450$ Å for $(D)_n$ clusters at $I=10^{16}-10^{18}\,W\,cm^{-2}$. The most important conclusion emerging from the results of Fig. 7 is that in the high intensity range of $I \geqslant 10^{17}-10^{19}\,W\,cm^{-2}$ and at a fixed value of the cluster radius, the $\langle \sigma v \rangle$ value for the NFDCE of a $(CD_4)_n$ cluster is considerably higher than the $\langle \sigma v \rangle$ value for the NFDCE of a $(D)_n$ cluster of the same size. For example, for $R_0=30$ Å the $\langle \sigma v \rangle$ value for NFDCE of $(CD_4)_n$ clusters is higher by a numerical factor of ~ 700 than for $(D)_n$ clusters at $I=10^{18}\,W\,cm^{-2}$. The R_0 fixed enhancement of the $\langle \sigma v \rangle$ values from $(CD_4)_n$ to $(D)_n$ is roughly given by the ratio of the $\bar{\alpha}$ parameters for the two families of clusters. This enhancement of $\langle \sigma v \rangle$ for NFDCE of deuterium containing heteroclusters, relative to $(D)_n$ homonuclear clusters of the same size (Fig. 7), reflects on energetic triggering and kinematic effects in the Coulomb explosion of heteroclusters, which will be manifested in the *dd* fusion yields.

The *dd* fusion reaction neutron yield Y per laser pulse is related to the $\langle \sigma v \rangle$ value by

$$Y=(1/2)\rho N(\bar{\ell}/\bar{v})\langle \sigma v \rangle, \tag{27}$$

where ρ is the neutron density, N is the number of deuterons in the reaction volume V_r, $\bar{\ell}$ is the mean path of deuterons inside the reaction volume, and $\bar{v}$ is the average velocity of the reactive deuterons. Adopting the experimental conditions of the Lawrence-Livermore group,[18,19] the following parameters were used: deuteron density $\rho=2\times10^{19}\,cm^{-3}$, number of deuterons $N=1.2\times10^{15}$, and mean free path $\bar{\ell}=0.016$ cm.[19]

Figure 8 portrays the calculated neutron yields for NFDCE of $(D)_n$ homonuclear clusters and $(CD_4)_n$ heteroclusters in the intensity range $I=10^{16}-10^{19}\,W\,cm^{-2}$, calculated for the geometry of the Lawrence-Livermore experimental conditions. The general laser intensity and cluster size dependence of Y (Fig. 8) are similar to those for the $\langle \sigma v \rangle$ data (Fig. 7) previously considered. In the higher intensity range $I=10^{17}-10^{19}\,W\,cm^{-2}$, the NFDCE of both the $(CD_4)_n$ and the $(D)_n$ clusters manifests the empirical size relation $Y \simeq \alpha \exp(-\beta/R_0)$, with $\beta=25$ at $I \geqslant 10^{17}\,W\,cm^{-2}$ for $(CD_4)_n$ and $\beta=44$ at $I=10^{16}-10^{18}\,W\,cm^{-2}$ for $(D)_n$. At a fixed value of R_0 and for $I \geqslant 10^{17}\,W\,cm^{-2}$, the ratio of the yields $Y[(CD_4)_n]/Y[(D)_n]$ is $50-10^3$, manifesting the marked enhancement of the NFDCE of $(CD_4)_n$ heteroclusters in comparison to the NFDCE of homonuclear $(D)_n$ clusters of the same size, which is due to energetic driving and kinematic effects in the NFDCE of heteroclusters.

A confrontation between simulation results and experiment[18] for the cluster size dependence of the yields of *dd* NFDCE of deuterium homonuclear clusters is of interest. Our simulation results for the neutron yields for NFDCE of deuterium clusters at $I=10^{18}\,\mathrm{W\,cm^{-2}}$ (Fig. 8) are systematically lower than the experimental results of the Lawrence-Livermore group[18] for the cluster size domain $R_0=25-55$ Å at $I=5\times10^{17}\,\mathrm{W\,cm^{-2}}$. In addition, our simulation results at $I=10^{18}\,\mathrm{W\,cm^{-2}}$ do not show the maximum in the neutron yield around $R_0\sim55$ Å, as experimentally observed by Zweiback *et al.*[18] The apparent maximum or onset of saturation of Y at $R_0\simeq55-60$ Å exhibited for the experimental data at $I=5\times10^{17}\,\mathrm{W\,cm^{-2}}$ (Ref. 18) does not seem to originate from the attainment of the boundary cluster size $(R_0)_I$ (Paper III and Sec. VI). This conclusion results from our estimates (Fig. 6) of $(R_0)_I\simeq145$ Å at $I=5\times10^{17}\,\mathrm{W\,cm^{-2}}$, which are considerably higher than the experimental value[18] of $R_0=55-60$ Å for the maximum or onset of saturation of the neutron yield. The deviations between our simulation results for fixed cluster sizes and the experimental data[18] may be partially due to the distribution of cluster sizes obtained under the experimental conditions.

Finally, we attempted to enquire what the nearly maximal values of $\langle\sigma v\rangle$ and of the neutron yields Y are for the NFDCE of assemblies of $(CD_4)_n$ heteroclusters and of $(D)_n$ homonuclear clusters at a given laser intensity in the intensity range $I=10^{16}-10^{19}\,\mathrm{W\,cm^{-2}}$. From the introduction and the analysis of the boundary (intensity dependent) cluster sizes $(R_0)_I$ for the attainment of the CVI domain (Sec. IV), we can infer that $(R_0)_I$ provides the nearly maximal cluster size for which effective outer ionization exists at a given I, which allows for effective Coulomb explosion. Increasing the cluster radius beyond $(R_0)_I$ will not result in an effective increase of the D^+ ion energies above $E_{D,av}=a(R_0)_I^2$. Using the data for $(R_0)_I$ (Fig. 6) and the corresponding $P(E)$ data simulated for these boundary radii in the intensity range $I=10^{16}-10^{19}\,\mathrm{W\,cm^{-2}}$ for both $(CD_4)_n$ and $(D)_n$ clusters, we calculated the parameters $\langle\sigma v\rangle_I$ and Y_I for these clusters. From the results of Fig. 9 we infer that the nearly maximal parameters $\langle\sigma v\rangle_I$ and Y_I for NFDCE vary over about ten orders of magnitude over the intensity range $I=10^{16}-10^{19}\,\mathrm{W\,cm^{-2}}$ with high values of $Y\simeq10^6-10^7$, being obtained for both $(CD_4)_n$ clusters [with $(R_0)_I=100$ Å at $I=10^{18}\,\mathrm{W\,cm^{-2}}$ and $(R_0)_I=250$ Å at $I=10^{19}\,\mathrm{W\,cm^{-2}}$] and $(D)_n$ clusters [with $(R_0)_I=204$ Å and $(R_0)_I=640$ Å at $I=10^{18}\,\mathrm{W\,cm^{-2}}$ and $I=10^{19}\,\mathrm{W\,cm^{-2}}$, respectively) in the high intensity range of $I=10^{18}-10^{19}\,\mathrm{W\,cm^{-2}}$. It is also instructive to note that these near-maximal values of $\langle\sigma v\rangle_I$ and Y_I at a fixed I result in somewhat higher values for NFDCE of $(D)_n$ homonuclear clusters than for $(CD_4)_n$ heteroclusters (Fig. 9). This optimization effect can be readily traced to considerably lower values of $(R_0)_I$ for $(CD_4)_n$ heteroclusters than for $(D)_n$ homonuclear clusters at a fixed laser intensity (Fig. 6).

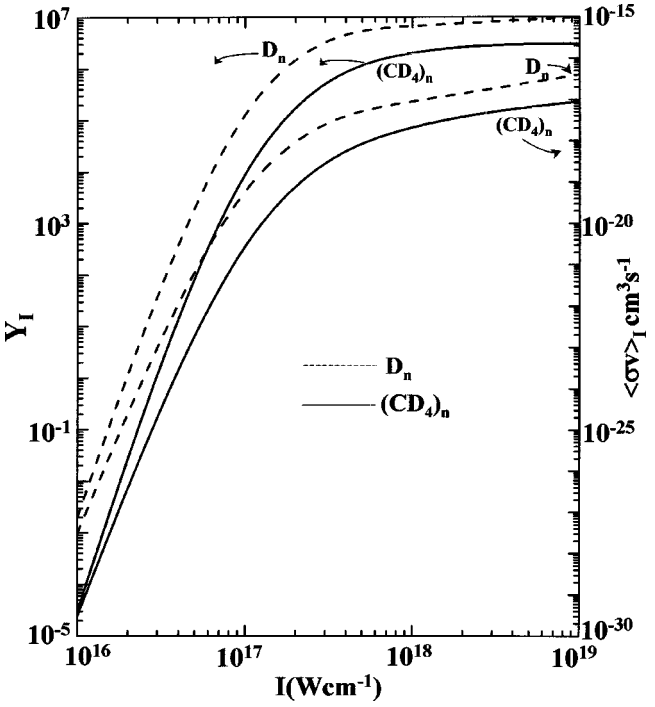

FIG. 9. Modeling of the optimization of the sizes of $(CD_4)_n$ and $(D)_n$ clusters at a fixed laser intensity (in the range $I=10^{16}-10^{19}\,\mathrm{W\,cm^{-2}}$) for the attainment of nearly maximal values of the kinetic parameters and the neutron yields per pulse. Calculations, based on Eqs. (21), (22), and (24)–(27), were performed for kinetic parameters (marked $\langle\sigma v\rangle_I$) and neutron yields (marked Y_I) for clusters of (intensity dependent) boundary radius $(R_0)_I$ (Fig. 6), with the corresponding D^+ energy distribution calculated for these boundary radii. In the high intensity range $I=10^{18}-10^{19}\,\mathrm{W\,cm^{-2}}$ the maximal attainable Y_I data [under the experimental conditions of the Lawrence-Livermore laboratory (Ref. 13)] are $Y_I\simeq10^6$ for $(CD_4)_n$ and $Y_I\simeq10^7$ for $(D)_n$.

VIII. CONCLUDING REMARKS

The dynamics and energetics of Coulomb explosion of highly charged heteroclusters produced by extreme multielectron ionization in ultraintense laser fields studied herein are richer than the characteristics of Coulomb instability of multicharged homonuclear clusters (Paper III). Some of the manifestations of the coupling between electron and nuclear dynamics in heteroclusters are qualitatively similar to those of homonuclear clusters (Paper III), exhibiting outer ionization with the depletion of the nanoplasma, screening effects of the nanoplasma (for $I\leqslant10^{17}\,\mathrm{W\,cm^{-2}}$), and the attainment of nearly complete CVI for $R_0\leqslant(R_0)_I$ at intensity I. Effects of parallel electron and nuclear dynamics of heteroclusters pertain to the early stages of the spatial expansion of distinct ions during outer ionization. The nuclear dynamics and energetics of Coulomb explosion of heteroclusters exhibit different phenomena. These features involve bimodal (or multimodal) dynamic and energetic patterns, due to the formation of two (or more) distinct ionic species in the Coulomb exploding heterocluster, i.e., different spatial expansion dynamics, different energetics, and different energy distributions of distinct ions, as well as kinematic effects. Some simple, but significant, features of the energetics of heterocluster Coulomb explosion are exhibited in energetic triggering effects due to the driving of the light D^+ or H^+ ions by the highly charged heavy ions, e.g., C^{4+} produced at $I=10^{16}-10^{18}\,\mathrm{W\,cm^{-2}}$ and C^{6+} produced at $I=10^{19}\,\mathrm{W\,cm^{-2}}$, which manifest the implications of the intensity dependent ionization level on the energetics. But

most interesting are kinematic effects of heterocluster Coulomb explosion, which are governed by the kinematic parameter η, Eq. (1). While $\eta=1$ for uniform Coulomb explosion under CVI conditions, e.g., for $(C^{6+}D_4^+)_n$, nonuniform Coulomb explosion is ubiquitous, e.g., for $(C^{q_C+}H_4^+)_n$ ($q_C=4,6$) or for $(C^{4+}D_4^+)_n$. Nonuniform Coulomb explosion ($\eta>1$) manifests an overrun effect of the light ions relative to the heavy ions, exhibiting the expansion of two spatially separated subclusters, with the light ions forming the outer subcluster, which is assembled mainly at the outer edge of the spatial distribution. In the extreme case of extremely heavy multicharged ions, e.g., Coulomb explosion of $(H^+I^{q+})_n$ ($q=7-35$) clusters, the light ions assemble in an expanding monolayer, which bears analogy to a ''soap bubble'' expanding under repulsive interactions.[47]

The implications of the kinematic effects on the energetics of nonuniform Coulomb explosion of heteroclusters were explored by deriving analytic expressions for the uniform case under CVI initial conditions. The cluster size scaling laws for the average energies $E_{j,\mathrm{av}}=aR_0^2$ and for the maximal energies $E_{j,\mathrm{M}}=(5a/3)R_0^2$, Eqs. (7) and (8), as well as the energy distribution, $P(E_j)\propto E_j^{1/2}$, Eq. (9), provides benchmark reference data for the uniform expansion case. The $E_{j,\mathrm{av}}\propto R_0^2$ scaling still holds for nonuniform expansion, with an increase of the coefficient a relative to the uniform case, Eq. (7), being due to kinematic overrun effects, with the coefficient a increasing with the increase of η. Kinematic effects result in isotope effects on the energetics of the light ions, with the enhancement of the average energies of the H^+ ions from $(C^{q_C+}H_4^+)_n$ relative to those of the $(C^{q_C+}D_4^+)_n$ ($q_C=4$ and 6) heteroclusters of the same size. This isotope effect is determined by the ratio of the kinematic parameters for the pair of Coulomb exploding heteroclusters. This isotope effect is counterintuitive, as on the basis of heuristic arguments one might have expected that the heavy D^+ ions will acquire a higher kinetic energy than the light H^+ ions. Furthermore, kinematic effects grossly modify the energy distributions $P(E_j)$ of the light ions, which deviate considerably from the uniform Coulomb collision case. The energy distributions of the light H^+ and D^+ ions are moderately narrow, being characterized by a width ΔE of $\Delta E/E_{\mathrm{H,av}}\simeq 0.3$ for H^+ ions and of $\Delta E/E_{\mathrm{D,av}}\simeq 0.4$ for D^+ ions, with the distributions peaking near the higher energy edge, manifesting the lowering of ΔE for the lighter isotope for a pair of size-selected heteroclustes of identical size.

The predicted features of nonuniform Coulomb explosion pertaining to the light ions average energies, energy distribution, and isotope effects should be confronted with experiment. Of considerable interest will be the average energies for the H^+ and D^+ ions, which were calculated herein for fixed cluster sizes and for which an isotope effect was predicted. Regarding the maximal energies of the light ions, for which the maximal energy of the D^+ ions is predicted to be higher than for the H^+ ions, the situation is somewhat more complex. In this case, the initial size distribution of the heteroclusters has to be taken into account. This heterocluster size distribution, which is commonly described in terms of a log-normal distribution, will contain a small, but finite, fraction of large ions, whose sizes considerably exceed the average heterocluster size and which will contribute to the appearance of light ions with very high energies. Accordingly, a direct comparison between theory and experiment for the maximal energy of the light ions requires the extension of our calculations, which were performed for fixed heterocluster sizes, to incorporate the heterocluster size distributions.

The foregoing analysis of the dynamics and energetics of Coulomb explosion of multicharged heteroclusters provides the conceptual basis for *dd* NFDCE of molecular heteroclusters of deuterium bound to heavy atoms originally advanced by us.[20,28] Our analysis (Sec. VII) established the marked enhancement of the NFDCE of $(CD_4)_n$ heteroclusters in comparison to the NFDCE of homonuclear $(D)_n$ clusters of the same size, which was attributed to energetic driving and kinematic effects in the NFDCE of heteroclusters. Dramatic energetic triggering effects of D^+ ions are expected to be manifested in Coulomb explosion of deuterium containing molecular heteroclusters of heavy atoms, e.g., mixed xenon-deuterium $(Xe)_m(D_2)_n$ heteroclusters, or iodine containing, i.e., $(DI)_n$ or $(CD_3I)_n$, heteroclusters. On the basis of recent studies of xenon clusters (Paper I) or of $(HI)_n$ heteroclusters[47] we expect that in the laser intensity range of $I=10^{18}\,\mathrm{W\,cm^{-2}}$, highly charged Xe^{26+} ions from $(Xe)_m(D_2)_n$, or I^{25+} ions from $(DI)_n$ or $(CD_3I)_n$ heteroclusters, will be produced by extreme multielectron ionization. On the basis of the CVI scaling law, Eq. (7), we infer that the Xe^{26+} or I^{25+} heavily charged energetic triggers will drive D^+ ions to a kinetic energy range, which is about fivefold higher than obtained by C^{4+} or C^{6+} ions, and which is about a numerical factor of ~ 30 higher than the kinetic energy of ions from totally ionized $(D_2)_n$ clusters of the same size. Accordingly, nuclear fusion in the D^+ energy domain of 100 keV [where *dd* nuclear fusion cross sections are large, i.e., $\sigma>10^{-26}\,\mathrm{cm^2}$ (Ref. 44)] can be accomplished.

ACKNOWLEDGMENTS

This research was supported by the Deutsche Forschungsgemeinschaft (SFB 450) and by the Binational German-Israeli James Franck program on laser-matter interactions.

APPENDIX A: UNIFORM COULOMB EXPLOSION OF MOLECULAR HETEROCLUSTERS

The structure of $(A_{k'}^{q_A+}B_k^{q_B+})_n$ clusters is described in terms of a spherical initial cluster with a radius R_0 (at $t=0$). The initial density $\rho_j[r_j(0)]$ of the ions of type j ($j=A$ or B), which are located at radii $\{r_j(0)\}$ from the cluster center, is uniform, i.e., $\rho_j[r_j(0)]=\rho_j$ at $r_j(0)\leqslant R_0$ and $\rho_j[r_j(0)]=0$ at $r_j\geqslant R_0$, for all j. The initial total molecular ion density is $\rho_{\mathrm{mol}}=\rho_j/k_j$, where k_j is the number of j-type atoms within the molecule. The initial total charge of the jth type ions within the sphere radius $r_j(0)(\leqslant R_0)$ is

$$Q_j[r_j(0)]=(4\pi/3)r_j(0)^3\rho_j q_j, \tag{A1}$$

where q_j is the individual charge of the jth ion and $q_{\mathrm{mol}}=\Sigma_{j'}q_{j'}$ is the molecular ion charge. The total initial ionic charge within the $r_j(0)$ sphere is

$$Q[r_j(0)]=\sum_{j'} Q_{j'}[r_j(0)], \tag{A2}$$

which takes the form

$$Q[r_j(0)]=(4\pi/3)r_j(0)^3\rho_{\mathrm{mol}}q_{\mathrm{mol}}. \tag{A3}$$

The Coulomb explosion, which preserves spherical symmetry, moves a jth type ion from $r_j(0)$ at $t=0$ to $r_j(t)$ at time t. The total charge of the jth ions within the radius $r_j(t)$ is $Q_j[r_j(t)]$. Uniform Coulomb explosion implies that the succession of the jth ion distances from the cluster center is preserved during those ion expansions obeying two conditions: (A) For any pair of ions of the same type j with initial distances $r_j'(0)$ and $r_j''(0)$, with $r_j''(0)>r_j'(0)$, the distances at time t are $r_j''(t)>r_j'(t)$. (B) For any pair of ions of different types j' and j'', with initial distances $r_{j''}(0)>r_{j'}(0)$, the expansion distances at any time t are $r_{j''}(t)>r_{j'}(t)$. Conditions (A) and (B) imply no overrun effects. For such a uniform (smooth) expansion, we expect that the total charge of the jth type ions $Q_j[r_j(t)]$ within the radius $r_j(t)$ is invariant with time, i.e., $Q_j[r_j(t)]=Q_j[r_j(0)]$, for all t. Accordingly, the total ionic charge within the radius $r_j(t)$ is

$$Q[r_j(t)]=Q[r_j(0)]. \tag{A4}$$

The kinetic energy $E_j[r_j(t);r_j(0)]$ of a j-type ion moving from $r_j(0)$ to $r_j(t)$ is the difference between the Coulomb potentials at these two distances,

$$E_j[r_j(t);r_j(0)]=\overline{B}Q[r_j(t)]q_j\left(\frac{1}{r_j(0)}-\frac{1}{r_j(t)}\right), \tag{A5}$$

where $\overline{B}=14.385\ \mathrm{eV\ \AA^{-1}}$. From Eqs. (A2)–(A5) we obtain

$$E_j[r_j(t);r_j(0)]=\overline{B}(4\pi/3)\rho_{\mathrm{mol}}q_{\mathrm{mol}}q_j[r_j(0)]^3 \times\left(\frac{1}{r_j(0)}-\frac{1}{r_j(t)}\right). \tag{A6}$$

Equation (A6) leads to Eq. (3).

APPENDIX B: DYNAMICS AND ENERGETICS OF UNIFORMLY EXPLODING HETEROCLUSTERS

The characteristic Coulomb explosion times τ_2, Eq. (4), for uniformly exploding heteroclusters (with m_j/q_j being identical for all j cluster atomic ions) under CVI conditions reveal the following features.

(1) Charge dependence and mass effects: $\tau_2\propto(m_j/q_jq_{\mathrm{mol}})^{1/2}$, exhibiting a reciprocal dependence on the square root of the product of atomic ions and molecular ion charges. For the mass effect $\tau_2\propto(m_j)^{1/2}$. Accordingly, for Coulomb explosion of a uniformly expanding heteronuclear cluster, with $m_j/q_j=$const for all ions, τ_2 is identical for the distinct ions.

(2) Dependence of the neutral cluster structure, with $\tau_2\propto(\rho_{\mathrm{mol}})^{-1/2}\propto(r_a)^{3/2}$, where r_a is the interconstituent. This result reflects on the lengthening of τ_2 for a larger size of the initial cluster constituents.

(3) Cluster size dependence: No cluster size dependence of τ_2 is expected. The absence of size scaling is expected to prevail for sufficiently large clusters where the continuum approximation for the derivation of Eq. (2) applies.

From the analysis of the energetics, Eqs. (7)–(9), for uniformly exploding clusters we infer the following.

(1) Cluster size dependence: Both $E_{j,\mathrm{M}}$ and $E_{j,\mathrm{av}}$ scale as R_0^2. The relation $E_{j,\mathrm{M}}$, $E_{j,\mathrm{av}}\propto R_0^2$ constitutes a divergent cluster size equation (Paper III).

(2) Charge dependence: The relation $E_{j,\mathrm{M}}$, $E_{j,\mathrm{av}}\propto q_{\mathrm{mol}}q_j$ is a consequence of the electrostatic energy in a multicharged cluster which underwent CVI.

(3) For the uniform Coulomb explosion of a heterocluster, which generates several distinct $\{j\}$ ions, the proportionality of the energies on q_j, with $m_j/q_j=$constant, implies proportionality of the energies on m_j for different kinds of ions in a heteronuclear cluster.

(4) Dependence on initial cluster configuration: $E_{j,\mathrm{M}}$, $E_{j,\mathrm{av}}\propto\rho_{\mathrm{mol}}\propto r_a^{-3}$, reflecting on the decrease of the ion energies for a larger size of the cluster initial constituents.

(5) Relation between maximal and average energies: The simple relation $E_{j,\mathrm{M}}/E_{j,\mathrm{av}}=5/3$ for each j ion is applicable.

(6) Specific dependence of the energies on the nature of the ion: The ratios of energies of different ions scale as the charges of these ions, i.e., $E_{j\mathrm{M}}/E_{j'\mathrm{M}}=E_{j\mathrm{av}}/E_{j'\mathrm{av}}=q_j/q_{j'}$. A uniformly expanding heteronuclear multicharged cluster ($q_j/m_j=$const for all j), inferred from points (3) and (5) above, implies that $E_{j\mathrm{M}}/E_{j'\mathrm{M}}=E_{j\mathrm{av}}/E_{j'\mathrm{av}}=m_j/m_{j'}$. Thus, different atomic ions manifest different energies, which are proportional both to their charges and to their masses. In the limit of uniform Coulomb explosion of a heteronuclear uniformly expanding cluster the number of the maximal energy values is equal to the number of the distinct ions in the exploding cluster.

(7) The energy distribution $P(E_j)\propto E_j^{1/2}$ for the jth ion, Eq. (9), is expected to be different for each type of distinct ion in the exploding cluster.

(8) Isotope effects on the energetics: For distinct homonuclear or heteronuclear clusters, which consist of distinct isotopic species and which manifest uniform Coulomb explosion, we expect that $E_{j,\mathrm{av}}$, Eq. (7), and $E_{j,\mathrm{M}}$, Eq. (8), are independent of the isotopic species. Thus the energetics of Coulomb explosion of $(\mathrm{H}^+)_n$, $(\mathrm{D}^+)_n$, and $(\mathrm{T}^+)_n$ clusters are expected to be identical (apart from minor isotope effects on ρ_{mol} and R_0). On the other hand, for isotopically substituted heteroclusters, e.g., $(\mathrm{C}^{4+}\mathrm{H}_4^+)_n$, $(\mathrm{C}^{4+}\mathrm{D}_4^+)_n$, and $(\mathrm{C}^{4+}\mathrm{T}_4^+)_n$ [where only the $(\mathrm{C}^{4+}\mathrm{T}_4^+)_n$ heterocluster corresponds to the uniform case], the $E_{j,\mathrm{av}}$ and $E_{j,\mathrm{M}}$ energies will manifest deviations from Eqs. (7) and (8), respectively, due to kinematic effects, and isotope effects on the energetics are expected. Also, isotope effects on $E_{j,\mathrm{av}}$ and $E_{j,\mathrm{M}}$ ($j=$H and D), arising from kinematic effects, will be exhibited for different ions from Coulomb explosion of an isotopically mixed single heterocluster, e.g., H^+ and D^+ ions from the nonuniform Coulomb explosion of $(\mathrm{C}^{4+}\mathrm{H}_2^+\mathrm{D}_2^+)_n$.

[1] T. Ditmire, R. A. Smith, J. W. G. Tisch, and M. H. R. Hutchinson, Phys. Rev. Lett. **78**, 3121 (1997).
[2] T. Ditmire, J. W. G. Tisch, E. Springate, M. B. Mason, N. Hay, J. P. Marangos, and M. H. R. Hutchinson, Phys. Rev. Lett. **78**, 2732 (1997).
[3] K. Kondo, A. B. Borisov, C. Jordan, A. McPherson, W. A. Schroeder, K. Boyer, and C. K. Rhodes, J. Phys. B **30**, 2707 (1997).

[4] M. Lezius, S. Dobosz, D. Normand, and M. Schmidt, Phys. Rev. Lett. **80**, 261 (1998).
[5] I. Last and J. Jortner, Phys. Rev. A **60**, 2215 (1999).
[6] I. Last and J. Jortner, Phys. Rev. A **62**, 013201 (2000).
[7] E. Springate, N. Hay, J. W. G. Tisch, M. B. Mason, T. Ditmire, M. H. R. Hutchinson, and J. P. Marangos, Phys. Rev. A **61**, 063201 (2000).
[8] K. Ishikava and T. Blenski, Phys. Rev. A **62**, 063204 (2000).
[9] K. J. Mendham, N. Hay, M. B. Mason, J. W. G. Tisch, and J. P. Marangos, Phys. Rev. A **64**, 055201 (2001).
[10] M. Schnürer, S. Ter-Avetisyan, H. Stiel, U. Vogt, W. Radloff, M. Kalashnikov, W. Sandner, and P. V. Nickles, Eur. Phys. J. D **14**, 331 (2001).
[11] C. Siedschlag and J. M. Rost, Phys. Rev. A **67**, 013404 (2003).
[12] V. Kumarappan, M. Krishnamurthy, and D. Mathur, Phys. Rev. A **67**, 043204 (2003).
[13] Y. Fukuda, K. Yamakawa, Y. Akahane, M. Aoyama, N. Inoue, H. Ueda, and Y. Kishimoto, Phys. Rev. A **67**, 061201 (2003).
[14] I. Last and J. Jortner, Z. Phys. Chem. (Munich) **127**, 975 (2003).
[15] S. Ter-Avetisyan, U. Vogt, H. Stiel, M. Schnürer, I. Will, and P. V. Nicles, J. Appl. Phys. **94**, 1 (2003).
[16] J. Schulz, H. Habnitz, T. Laarmann, S. Gürtler, W. Laasch, A. Swiderski, Th. Möller, and A. A. B. de Castro, Nucl. Instrum. Methods Phys. Res. A **507**, 572 (2003).
[17] A. Santra and Ch. M. Greene, Phys. Rev. Lett. **91**, 233401 (2003).
[18] J. Zweiback, R. A. Smith, T. E. Cowan, G. Hays, K. B. Wharton, V. P. Yanovsky, and T. Ditmire, Phys. Rev. Lett. **84**, 2634 (2000).
[19] J. Zweiback, T. E. Cowan, R. A. Smith, J. H. Hurtlay, R. Howell, C. A. Steinke, G. Hays, K. B. Wharton, J. K. Krane, and T. Ditmire, Phys. Rev. Lett. **85**, 3640 (2000).
[20] I. Last and J. Jortner, Phys. Rev. Lett. **87**, 033401 (2001).
[21] I. Last and J. Jortner, Phys. Rev. A **64**, 063201 (2001).
[22] J. Jortner and I. Last, ChemPhysChem **3**, 845 (2002).
[23] M. Eloy, R. Azambuja, and J. Mendonça, Phys. Plasmas **8**, 1084 (2001).
[24] P. B. Parks, T. E. Cowan, R. B. Stephens, and E. M. Campbell, Phys. Rev. A **63**, 063203 (2002).
[25] R. W. Madison, P. K. Patel, M. Allen, D. Price, R. Fitzpatrick, and T. Ditmire, Phys. Plasmas **11**, 1 (2004).
[26] S. Sakabe, S. Shimizu, M. Hashida *et al.*, Phys. Rev. A **69**, 023203 (2004).
[27] V. Kumarappan, M. Krishnamurthy, and D. Mathur, Phys. Rev. A **67**, 063207 (2003).
[28] I. Last and J. Jortner, J. Phys. Chem. A **106**, 10877 (2002).
[29] G. Grillon, Ph. Balcou, J.-P. Chambaret *et al.*, Phys. Rev. Lett. **89**, 065005 (2002).
[30] T. Ditmire, Phys. Rev. A **57**, R4094 (1998).
[31] V. P. Krainov and M. B. Smirnov, Phys. Rep. **370**, 237 (2002).
[32] I. Last and J. Jortner, J. Chem. Phys. **120**, 1336 (2004) (Paper I).
[33] I. Last and J. Jortner, J. Chem. Phys. **120**, 1348 (2004) (Paper II).
[34] T. Ditmire, J. W. G. Tisch, E. Springate, M. B. Mason, N. Hay, R. A. Smith, J. Marangos, and M. H. R. Hutchinson, Nature (London) **386**, 54 (1997).
[35] C. Siedschlag and J. M. Rost, Phys. Rev. A **67**, 013404 (2003).
[36] J. Levin, H. Feldman, A. Baer, D. Ben-Hamu, O. Heber, D. Zeifman, and Z. Vager, Phys. Rev. Lett. **81**, 3347 (1998).
[37] S. Chelkowski, P. B. Corkum, and A. D. Bandrauk, Phys. Rev. Lett. **82**, 3416 (1999).
[38] D. A. Card, E. S. Wisniewski, D. E. Folmer, and A. W. Castleman, Jr., J. Chem. Phys. **116**, 3554 (2002).
[39] D. E. Folmer, L. Poth, E. S. Wisniewski, and A. W. Castleman, Jr., Chem. Phys. Lett. **287**, 1 (1998).
[40] A. E. Kaplan, B. Y. Dubetsky, and P. L. Shkolnikov, Phys. Rev. Lett. **91**, 143401 (2003).
[41] I. Last, I. Schek, and J. Jortner, J. Chem. Phys. **107**, 6685 (1997).
[42] I. Last and J. Jortner, J. Chem. Phys. **121**, 3030 (2004) (Paper III).
[43] P. M. Echenique, P. M. Manson, and R. M. Ritchi, Phys. Rev. Lett. **64**, 1413 (1990).
[44] D. J. Rose and M. Clark, Jr., *Plasmas and Controlled Fusion* (MIT, Massachusetts, 1961).
[45] L. A. Artsimovich, *Controlled Thermonuclear Reactions* (Gordon and Breach Science, New York, 1964).
[46] S. Gladstone and R. H. Lovberg, *Controlled Thermonuclear Reactions* (Van Nostrand, New York, 1960).
[47] I. Last and J. Jortner (unpublished).